Quaternary Science Reviews 25 (2006) 2729–2748

Pleistocene lake outburst floods and fan formation along the eastern Sierra Nevada, California: implications for the interpretation of intermontane lacustrine records

Douglas I. Benn[a,b,*], Lewis A. Owen[c], Robert C. Finkel[d], Samuel Clemmens[e]

[a] *School of Geography and Geosciences, University of St. Andrews, St. Andrews KY16 9AL, UK*
[b] *Department of Geology, UNIS, PO Box 156, N-9171 Longyearbyen, Norway*
[c] *Department of Geology, University of Cincinnati, Cincinnati, OH 45221-0013, USA*
[d] *Center for Accelerator Mass Spectrometry, Lawrence Livermore National Laboratory, Livermore, CA 94550, USA*
[e] *Institute of Geography and Earth Sciences, University of Wales, Aberystwyth SY23 3DB, UK*

Received 10 June 2005; accepted 5 February 2006

Abstract

Variations in the rock flour fraction in intermontane lacustrine sediments have the potential to provide more complete records of glacier fluctuations than moraine sequences, which are subject to erosional censoring. Construction of glacial chronologies from such records relies on the assumption that rock flour concentration is a simple function of glacier extent. However, other factors may influence the delivery of glacigenic sediments to intermontane lakes, including paraglacial adjustment of slope and fluvial systems to deglaciation, variations in precipitation and snowmelt, and lake outburst floods. We have investigated the processes and chronology of sediment transport on the Tuttle and Lone Pine alluvial fans in the eastern Sierra Nevada, California, USA, to elucidate the links between former glacier systems located upstream and the long sedimentary record from Owens Lake located downstream. Aggradation of both fans reflects sedimentation by three contrasting process regimes: (1) high magnitude, catastrophic floods, (2) fluvial or glacifluvial river systems, and (3) debris flows and other slope processes. Flood deposits are represented by multiple boulder beds exposed in section, and extensive networks of large palaeochannels and boulder deposits on both fan surfaces. Palaeohydrological analysis implies peak discharges in the order of 10^3–$10^4\,m^3\,s^{-1}$, most probably as the result of catastrophic drainage of ice-, moraine-, and landslide-dammed lakes. Cosmogenic radionuclide surface exposure dating shows that at least three flood events are represented on each fan, at 9–13, 16–18 and 32–44 ka (Tuttle Fan); and at ~23–32, ~80–86 ka, and a poorly constrained older event (Lone Pine Fan). Gravels and sands exposed in both fans represent fluvial and/or glacifluvial sediment transport from the Sierra Nevada into Owens Valley, and show that river systems incised and reworked older sediment stored in the fans. We argue that millennial-scale peaks in rock flour abundance in the Owens Lake core reflect (1) fluctuations in primary subglacial erosion in the catchments in response to glacier advance–retreat cycles; (2) short-lived pulses of sediment delivered directly by catastrophic flood events; and (3) sediment released from storage in alluvial fans by fluvial and glacifluvial incision and reworking. As a result of this complexity the coarse sediment peaks in lake deposits may not simply reflect periods of increased glaciation, but likely also reflect changes in sediment storage and flux controlled by paraglacial processes. Current dating evidence is inadequate to allow precise correlation of individual flood or incision events with the Owens Lake rock flour record, although given the widespread occurrence of flood deposits in fans along the eastern margins of the Sierra Nevada, it is clear that fan deposition and incision played a very important role in modulating the delivery of glacigenic sediment to Owens Lake.

1. Introduction

Mountain glaciers are sensitive indicators of climate change, and records of their fluctuations can be used to reconstruct palaeoclimate in regions where other forms of evidence are lacking. The geomorphological record of

*Corresponding author. Tel.: +47 79023367; fax: +47 79023301.
E-mail address: Doug.Benn@unis.no (D.I. Benn).

0277-3791/$ - see front matter © 2006 Elsevier Ltd. All rights reserved.
doi:10.1016/j.quascirev.2006.02.018

glacier fluctuations, however, is very incomplete, because later advances tend to destroy evidence of less extensive earlier ones (Gibbons et al., 1984; Kirkbride and Brazier, 1998). More complete records can be obtained from cores recovered from lacustrine sediments in intermontane basins, provided glacier advances can be identified from proxy data. For example, rock flour components in lacustrine sediments recovered from Owens Lake, California, have been used to determine the timing of glacier advances in the adjacent Sierra Nevada (Benson et al., 1996; Bischoff and Cummins, 2001; Benson, 2004), based on the assumption that maximum sediment fluxes from glaciated basins occur during glacial maxima. This assumption, however, needs to be tested. Numerous studies have shown that the highest sediment yields from glaciated basins occur not when glaciers are at their maximum extent, but during or following deglaciation, as the landscape adjusts from glacial to non-glacial conditions (Church and Ryder, 1972; Ballantyne 2002). This *paraglacial* period of enhanced sediment flux may lag glacial maxima by several centuries, or even millennia in the case of large basins (Church and Slaymaker, 1989; Harbor and Warburton, 1993). If peak sediment yields occur during the paraglacial period, then maximum glacigenic sediment input to lacustrine basins may be offset substantially from the coldest climatic intervals.

Accelerated sediment flux during the paraglacial period can be attributed to the availability of unconsolidated sediments on newly deglaciated terrain, and/or abundant meltwater during glacier recession (Ballantyne and Benn, 1996; Ballantyne, 2002). Additionally, in high-relief mountain environments, glacier thinning and recession commonly results in the ponding of lakes behind large lateral–frontal moraines, which are prone to catastrophic drainage (Benn et al., 2004). Glacier lake outburst floods (GLOFs) can transport large volumes of sediment derived from breached moraines and incised flood tracks (Lliboutry, 1977; Evans and Clague, 1994). Numerous GLOFs have occurred during recent glacier recession from late Holocene maxima in the North American Cordillera, the Himalaya, the Andes, and other high mountain regions (Jarrett and Costa, 1986; Vuichard and Zimmerman, 1986; O'Conner and Costa, 1993; Yamada, 1998; Richardson and Reynolds, 2000; Clague and Evans, 2000; O'Conner et al., 2001, 2002; Cenderelli and Wohl, 2003), and can be expected to have played an important role in sediment transport during earlier phases of deglaciation. Potentially unstable lakes can also form if ice expansion in one catchment blocks drainage from another, increasing the likelihood of GLOFs during periods of glacier advance (e.g. Vivian, 2001). Additionally, large amounts of sediment can be transported and deposited during the drainage of lakes dammed by rock avalanches and other slope failures, which may be especially frequent during the paraglacial period (Owen and Derbyshire, 1993; Ballantyne, 2002).

Transfer of sediment into intermontane lake basins from glacial and paraglacial sources is typically mediated through piedmont alluvial fans. Therefore, the sediment archive in such fans has the potential to yield important information on the processes and timing of sediment transfer between glacial, paraglacial, and lacustrine systems, which can be used to test the idea that glacigenic sediment peaks in lake cores coincide with glacial maxima. In this paper, we investigate glacial sediments and alluvial fans in the eastern Sierra Nevada, California, in two catchments that drain into Owens Lake, where long records of rock flour inputs are available. We use detailed geomorphological maps and logs of sediment exposures, in combination with cosmogenic radionuclide surface exposure dating (SED) to (1) determine the relative importance of glacifluvial, paraglacial and non-glacial sediment transport processes on the alluvial fans; (2) to develop improved chronologies of glacier fluctuations and fan development in the catchments; and (3) consider the implications for interpretation of the sediment record in Owens Lake and similar intermontane lacustrine basins.

2. Study area

Owens Lake occupies the floor of Owens Valley, a major north–south oriented graben near the western margin of the Basin and Range province (Fig. 1). The valley is bounded on the west by the Sierra Nevada, which rise steeply from the valley margins at ~1800 m to over 4000 m above sea level (asl) at the range crest, culminating in Mount Whitney (4416 m). At present, the Sierra Nevada contain numerous small niche glaciers, debris-mantled glaciers and rock glaciers at altitudes over 3600 m (Guyton, 1998). During the Wisconsin glaciation, glaciers extended to the range front, where they deposited large lateral–frontal moraine complexes (Porter et al., 1983; Clark et al. 2003; Kaufman et al., 2004, Fig. 1). The last major expansion of Sierran glaciers (the Tioga stage) occurred 25,000–15,000 years ago, during which time multiple moraines were formed in some localities (Phillips et al., 1996; Kaufman et al., 2004). Cosmogenic radionuclide dates on older moraines (Tahoe and Pre-Tahoe) show considerable spread, and the timing of pre-Tioga glaciations in the Sierra Nevada is not as well known as later

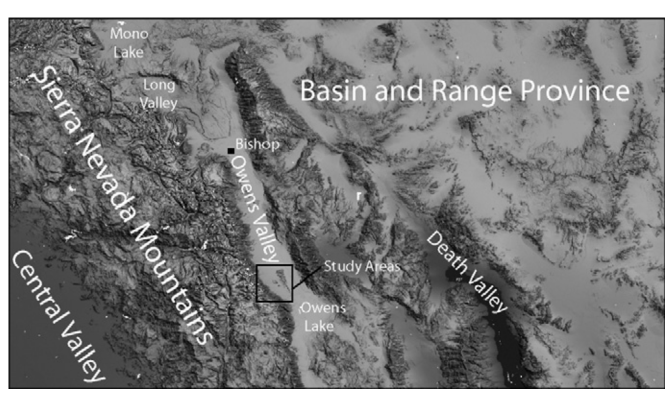

Fig. 1. Location map.

events. The eastern side of Owens Valley is bounded by the White and Inyo Mountains which rise to altitudes of ~2500–~4000 m asl. These mountains are currently unglaciated and supported restricted local glaciers during the Pleistocene.

Owens Lake is now a dry playa due to human water diversion, but historically was a perennial closed lake maintained against evaporative losses by river inflow (Reisner, 1986). During wet intervals of the Quaternary, the lake rose to the level of a spillway at the southern end, where it connected with a series of lakes extending eastward into Death Valley (Smith and Street-Perrott, 1983). Long sediment cores from Owens Lake have yielded important records of environmental change (Smith and Bischoff, 1997; Benson, 2004). A glacial rock flour component in Owens Lake sediments was first identified by Newton (1991), and subsequent analyses have documented fluctuations in rock flour abundance using total organic carbon (TOC), magnetic susceptibility (MS χ in Fig. 2) and chemical composition of the non-carbonate clay-sized fraction (CC) (Bischoff et al., 1997; Menking, 1997; Benson et al., 1998; Bischoff and Cummins, 2001). TOC tends to be inversely related to rock flour abundance, because the organic content of lake sediments is diluted by clastic inputs, and organic productivity is reduced in turbid and/or cold conditions. Benson et al. (1998) argued that minima in TOC provide evidence for 17 stades in the period from 53 to ~17.5 ka BP, when desiccation of Owens Lake occurred (Fig. 2). The broad minimum in TOC beginning at ca 27 ka, marking the Tioga glaciation, lacks the short-term fluctuations characteristic of the earlier record, suggesting that TOC may provide a less sensitive record of short-term glacier oscillations during full glacial conditions (when organic productivity is very low and rock flour yield is high) than when glaciers are less extensive (Benson et al., 1998). MS, recording relative abundance of Sierran magnetite and its weathering product greigite, exhibits many of the same peaks seen in the TOC record, although between ~45 and 30 ka they tend to be of low amplitude. Additionally, numerous sharp, short-lived spikes occur during the Tioga interval, superimposed on an overall falling trend (Fig. 2). These spikes may represent repeated pulses of magnetite into Owens Lake, although interpretation of the record is complicated by diagenetic and other factors. Bischoff and Cummins (2001) directly reconstructed rock flour abundance using concentrations of Na and Ca, inferred to derive solely from glacially eroded plagioclase from the Sierra Nevada. This record shares many of the characteristics of the TOC and MS proxies, including the occurrence of short-lived spikes during the Tioga.

Along both sides of Owens Valley, large coalescing piedmont fans extend from the mountains to the valley floor. Fans descending from the non-glaciated White and Inyo Mountains are typical of those in the south-western USA, consisting of thin-bedded debris flows and flash-flood deposits (Beaty, 1990; Blair and McPherson, 1998; Blair, 2002). In contrast, the fans on the Sierra Nevada side are very different in character, with surfaces littered with abundant massive boulders and traversed by systems of large, flat-floored channels. Whipple and Dunne (1992) and Bierman et al. (1995) have argued that the Sierran fans reflect deposition by large debris flows not necessarily associated with periods of glaciation. Blair (2001, 2002) conducted detailed studies of the Lone Pine and Tuttle fans north-west of Owens Lake (Fig. 3), and concluded that both were deposited by catastrophic GLOFs from moraine- or ice-dammed lakes. Blair argued that each fan contains evidence for a single, but multi-stage flood event post-dating the main stage of the Tioga glaciation. Bierman et al. (1995), however, recognised and dated four distinct surfaces on the Lone Pine fan, each of which has abundant large boulders on its surface. The oldest surface, Qg1, is heavily weathered, whereas Qg3 is fresher and characterised by numerous channels flanked by levées of large granodiorite boulders. The third fan surface is located ~8 km east of the range front, where Lone Pine Creek cuts through a gap in the Alabama Hills, and was termed the 'faulted fan' by Bierman et al. (1995) because its lower part

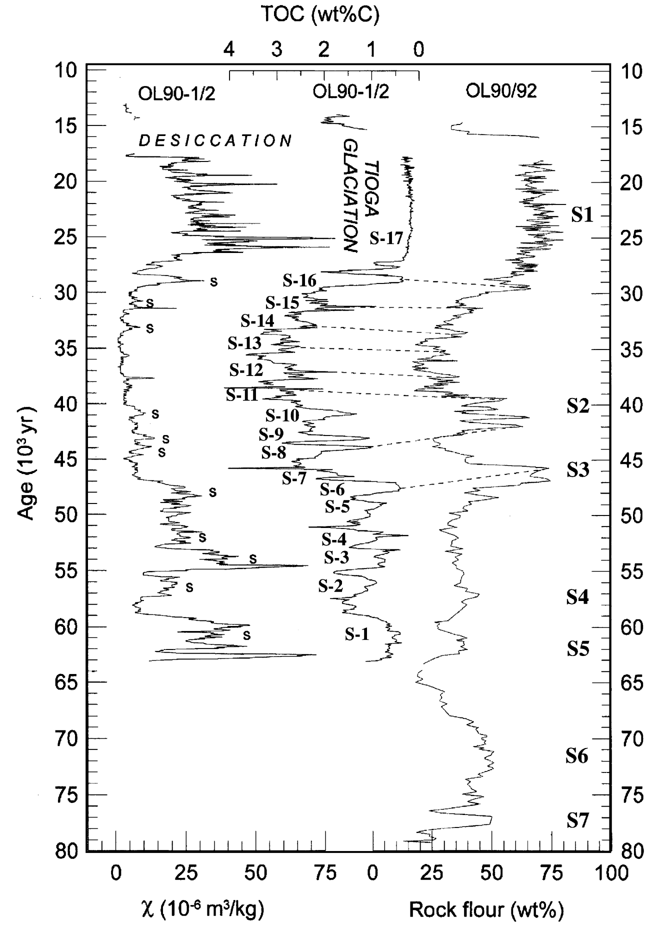

Fig. 2. Proxy records of rock flour abundance from Owens Lake (from Benson, 2004). S: 'Alpine stades' identified by Benson (2004); S-1–S-17: stades defined by Benson et al. (1998); S1–S7: major stades recognised by Bischoff and Cummins (2001).

has been displaced up to 6 m vertically by movement along the Lone Pine Fault. The final surface, Qg4, flanks the margins of Lone Pine Creek and is inset up to 20 m below Qg3. Cosmogenic radionuclide SED dates obtained by Bierman et al. (1995) from boulders on each of the fan surfaces are shown in Fig. 4, based on the revised production rates of Stone (2000). The dating evidence indicates that the Lone Pine fan has a complex history of aggradation and incision, and may record multiple GLOF events widely separated in time. If true, this interpretation could have important implications for the interpretation of the rock flour record from Owens Lake.

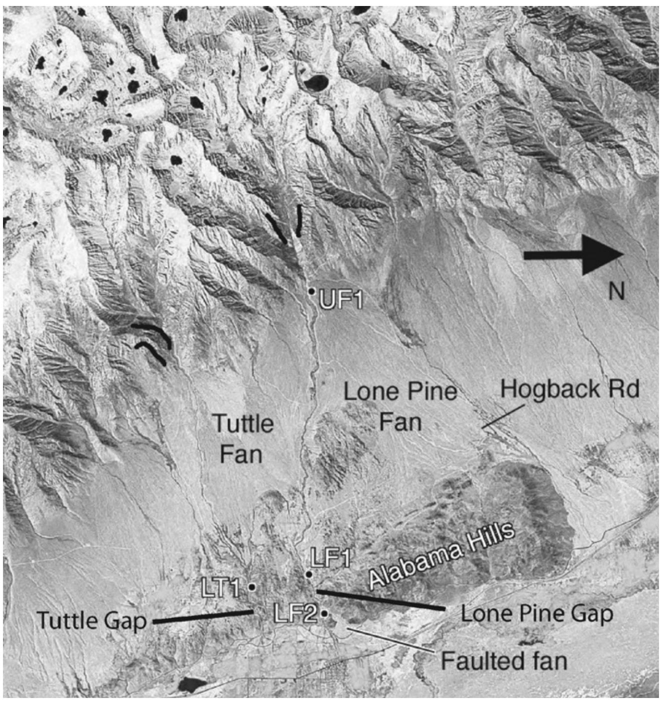

Fig. 3. Map of Lone Pine and Tuttle fans, showing the location of logged exposures. Moraines in the Tuttle and Lone Pine catchments are indicated by bold lines.

In this study, we re-examine the Lone Pine and Tuttle fans, and their relationship with (1) moraines located upstream and (2) the sediment record from Owens Lake downstream. In particular, we address the question of whether the fans preserve evidence of multiple GLOFs, and investigate the role of other, non-catastrophic processes in fan development and sediment transfer.

3. Methods

3.1. Geomorphology and sedimentology

Moraine distribution and fan-surface morphology were mapped in the field and from aerial photographs at a scale of approximately 1:25,000. Logs were made of selected sediment exposures to establish fan stratigraphy and sedimentological characteristics. Lithofacies were classified in the field on the basis of grain size, sorting, internal structures, and geometry, and grouped into lithofacies associations on the basis of the unit and bounding surface architecture. Palaeovelocity and discharge estimates were made from surveyed channel geometry and boulder dimensions at several locations, using the methods of Mears (1979) and Costa (1983).

3.2. Surface exposure dating

The timing of moraine formation and fan deposition relative to the Owens Lake record was established by SED using the concentration of ^{10}Be in boulders. The precision of SED depends on two major sources of uncertainty:

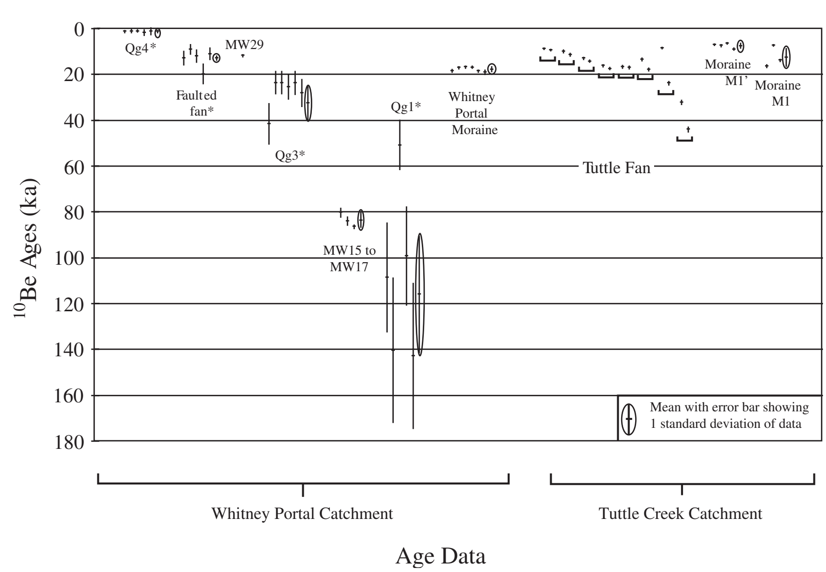

Fig. 4. Beryllium-10 terrestrial cosmogenic nuclide surface exposure dates on moraine and fan surfaces in the Lone Pine and Tuttle catchments. The ^{10}Be dates on Qg1, Qg3, Qg4 and the Faulted Fan (* starred) are scaled from Bierman et al. (1995) (cf. text). Note–Bierman et al.'s (1995) ^{26}Al dates are not plotted on this figure. Paired samples on the Tuttle fan are highlighted by the small square brackets.

estimates of the production rate of ^{10}Be and geologic processes. Production rate uncertainty is essentially a consequence of the paucity of calibration sites, and the surface exposure dates published by Bierman et al. (1995) incorporated production rate uncertainty of $\pm 20\%$. Since Bierman et al.'s (1995) paper was published the production rate for ^{10}Be has been refined. To allow a valid comparison between our new data and that of Bierman et al. (1995), the published ages were modified to account for improvements in estimates of the ^{10}Be production rate since 1995. We were not able to recalculate the Bierman et al. (1995) ages from primary sample data; therefore we chose simply to scale the published ages from a production rate of 6.03 at/g SiO_2-y to an instantaneous modern production rate of 5.44 at/g SiO_2-y. 5.44 at/g SiO_2-y is the production rate required by the geomagnetically corrected age-method described in Farber et al. (2005) and is based on the scaling method of Stone (2000). We estimate that these scaled ages may be biased by about 10–15% compared to ages calculated from primary data. The uncertainties quoted in our recalculation include only analytical uncertainty. The uncertainty in production rate has not been incorporated, although this may be in the order of $\sim$10% ($\pm$5%).

The geologic uncertainty results from several factors: inheritance of ^{10}Be in previously exposed surfaces; weathering of surfaces; shielding due to burial by sediment and/or snow; and, for samples taken from boulders, the possibility that toppling has occurred since boulder deposition. Our limiting exposure ages are calculated assuming no erosion. For weathering rates of 1–5 m Ma^{-1}, typical for the Sierra Nevada Mountains (Small et al., 1997; Zehfuss et al., 2001), an exposure age of 10 ka, would underestimate the true age by 1–4%; an age of 20 ka, by 2–9%; an age of 50 ka, by 4–20%; an age of 100 ka, by 10–36%; and an age of 200 ka, by 15–54%. Consideration of the dispersion of dates from deposit surfaces allows a qualitative assessment of the potential likelihood of spurious ages due to weathering, exhumation, toppling of boulders, and/or inheritance of terrestrial cosmogenic nuclides (TCNs) from derived boulders. For example, a broad spread of ages from a single deposit suggests progressive exhumation of boulders from beneath sediment cover or high incidence of inheritance, whereas old outliers from otherwise clustered dates indicate the likelihood of inheritance (Putkonen and Swanson, 2003).

Samples for SED were collected by chiselling off $\sim$500 g of rock from the upper surfaces of granodiorite boulders along moraine crests, and on levées and debris lobes on alluvial fans. Locations were chosen where there was no apparent evidence of exhumation or slope instability. The largest boulders were chosen to reduce the possibility that boulders may have been covered with snow for significant periods (several months) of the year. To provide a check on the reproducibility of the dating and to check for the possibility of inheritance of TCNs, several boulders were sampled from the moraine ridges and, where possible, duplicate boulders were collected at each sampling location on the alluvial fans. The degree of weathering and the site conditions for each boulder were recorded. Topographic shielding was determined by measuring the inclination from the boulder site to the top of the surrounding mountain ridges and peaks.

Following crushing and sieving, quartz was separated from the 250–500 μm size fraction of each sample using the method of Kohl and Nishiizumi (1992). The hydroxides were oxidised by ignition in quartz crucibles. BeO was then mixed with Nb metal prior to determination of the ^{10}Be/^{9}Be ratios by accelerator mass spectrometry at the Center for Accelerator Mass Spectrometry in the Lawrence Livermore National Laboratory. Isotope ratios were compared to ICN ^{10}Be standards prepared by K. Nishiizumi (pers. comm. 1995) using a ^{10}Be half-life of 1.5×10^6 yr.

The measured isotope ratios were converted to ^{10}Be concentrations in quartz using the total Be in the samples and the sample weights. Radionuclide concentrations were then converted to zero-erosion exposure ages using the scaling method of Stone (2000) and were corrected for geomagnetic field variations as described in Farber et al. (2005).

4. Moraine morphology and chronology

4.1. Lone pine creek

A prominent lateral moraine descends obliquely across the mountainside above the Whitney Portal road to the north of Lone Pine Creek, terminating at ca 2400 m asl (Fig. 3). Eastward of the moraine, in situ morainic sediments (predominantly diamicts with thin sand interbeds) extend along the valley side for a further $\sim$350 m. These sediments interdigitate with laterally extensive sets of cross-bedded and plane-bedded sands, which are up to 6 m thick. The presence of undeformed fluvial sediments banked against a steep hillside 150 m above the valley floor indicates that they were deposited between the hillside and a continuation of the lateral moraine, now lost to erosion. Modern analogues of this situation are provided by fluvial infills of troughs (''ablation valleys'') alongside moraines in the Himalaya and other high mountain environments (Owen and Derbyshire, 1989; Benn et al., 2004). Reworked diamicts containing glacially shaped clasts can be traced for a further 250 m downvalley beyond the in situ sediments.

A large lateral moraine with a similar gradient and altitudinal range occurs on the opposite hillside, on the south side of the Meysan valley (Fig. 3). Additionally, small moraine fragments occur at ca 2400 m asl on the spur between the Lone Pine and Meysan valleys, below which a degraded medial moraine descends the spur crest to the valley confluence. The evidence indicates that confluent glaciers descended from the Meysan Creek and Lone Pine Creek catchments, and extended at least 600 m beyond the present downvalley limit of the north lateral moraine.

On geomorphological evidence, it is not possible to determine whether the glacier terminus was enclosed by a continuous moraine loop, or whether it had an 'open' front with free meltwater drainage through a gap between lateral moraines. Both 'open' and 'closed' termini are found on modern debris-covered glaciers in the Himalaya and elsewhere (Owen and Derbyshire, 1989; Benn and Owen, 2002; Benn et al., 2004).

Five boulders on the crest of the north lateral ('Whitney Portal') moraine were sampled for SED, one of which provided two duplicate samples collected from the same rock surface, but spaced ~1 m apart (MW 1–5B, Table 1; Fig. 4). The dates are tightly clustered, with a mean of 17.8 ka, which corresponds closely with the date of the Tioga maximum advance elsewhere in the Sierra Nevada (James et al., 2002; Kaufman et al., 2004). Smaller moraines are inset within the Tioga lateral moraines in both the Lone Pine Creek and Meysan Creek valleys. The inset moraines are generally degraded, and prone to continuing deposition by rockfall from the steep overlying

Table 1
Sample and isotopic data, and ^{10}Be ages for boulders dated in this study

Sample number	Latitude and Longitude	Altitude (m)	Landform	Correction for topographic shielding	Be-10 concentration 10^5 at/g SiO_2[a]	Be-10 age (ka)
Tuttle fan						
MW12	36° 33.899′ N/118° 09.716′ W	1818	Levee on alluvial fan surface	0.99	1.60±0.06	8.8±0.3
MW13	36° 33.854′ N/118° 09.666′ W	1819	Levee on alluvial fan surface	1.00	1.73±0.05	9.4±0.3
MW22	36° 34.027′ N/118° 09.273′ W	1755	Debris lobe on alluvial fan surface	1.00	1.99±0.09	11.4±0.5
MW23	36° 34.045′ N/118° 09.256′ W	1749	Debris lobe on alluvial fan surface	1.00	1.72±0.10	9.9±0.6
MW26	36° 33.838′ N/118° 10.332′ W	1885	Levee on alluvial fan surface	0.99	2.43±0.08	13.0±0.4
MW27	36° 33.825′ N/118° 10.333′ W	1884	Levee on alluvial fan surface	0.99	2.69±0.09	14.3±0.5
MW10	36° 33.704′ N/118° 10.118′ W	1898	Levee on alluvial fan surface	1.00	3.38±0.09	17.4±0.5
MW11	36° 33.695′ N/118° 10.134′ W	1904	Levee on alluvial fan surface	1.00	3.13±0.08	16.2±0.4
MW24	36° 34.136′ N/118° 09.660′ W	1784	Boulder train on alluvial fan surface	1.00	2.92±0.09	16.7±0.5
MW25	36° 34.130′ N/118° 09.664′ W	1786	Boulder train on alluvial fan surface	1.00	3.07±0.11	17.1±0.6
MW30	36° 35.683′ N/118° 07.336′ W	1431	Alluvial fan surface	1.00	1.85±0.08	13.4±0.6
MW31	36° 35.673′ N/118° 06.775′ W	1386	Alluvial fan surface	1.00	2.38±0.09	17.8±0.7
MW32	36° 34.843′ N/118° 09.790′ W	1697	Alluvial fan surface	1.00	1.42±0.06	8.5±0.4
MW33	36° 34.841′ N/118° 09.784′ W	1697	Alluvial fan surface	1.00	4.08±0.12	23.8±0.7
MW14	36° 34.048′ N/118° 09.219′ W	1747	Levee on alluvial fan surface	1.00	8.29±0.20	44.0±1.1
MW21	36° 34.048′ N/118° 09.217′ W	1743	Levee on alluvial fan surface	1.00	5.81±0.16	32.1±0.9
Lone Pine fan just west of the Alabama Hills						
MW29	36° 35.701′ N/118° 08.022′ W	1488	Alluvial fan surface	1.00	1.70±0.07	12.6±0.5
Old fan surface nr. Moffat Ranch Rd at northern end of the Alabama Hills (Qg1)						
MW15	36° 40.766′ N/118° 07.612′ W	1226	Degraded alluvial fan surface	1.00	10.14±0.24	80.3±1.9
MW16a	36° 40.760′ N/118° 07.584′ W	1225	Degraded alluvial fan surface	1.00	10.59±0.22	84.0±1.8
MW17	36° 40.642′ N/118° 07.648′ W	1232	Degraded alluvial fan surface	1.00	10.94±0.10	86.4±7.7
Whitney Portal Moraine						
MW1	36° 35.504′ N/118° 13.559′ W	2448	Moraine crest	0.97	5.07±0.13	18.4±0.5
MW2	36° 35.510′ N/118° 13.535′ W	2448	Moraine crest	0.97	4.61±0.12	17.0±0.4
MW3	36° 35.515′ N/118° 13.509′ W	2460	Moraine crest	0.97	4.58±0.12	16.8±0.4
MW4	36° 35.520′ N/118° 13.484′ W	2444	Moraine crest	0.97	4.56±0.11	16.9±0.4
MW5A	36° 35.527′ N/118° 13.453′ W	2434	Moraine crest	0.97	4.99±0.12	18.5±0.5
MW5B	36° 35.527′ N/118° 13.453′ W	2434	Moraine crest	0.97	5.12±0.22	19.0±0.8
Tuttle moraine (M1′)						
MW34	36° 33.128′ N/118° 11.507′ W	2234	Moraine crest	0.96	1.62±0.07	7.1±0.3
MW35	36° 33.127′ N/118° 11.507′ W	2229	Moraine crest	0.96	1.70±0.09	7.4±0.4
MW36	36° 33.115′ N/118° 11.538′ W	2241	Moraine crest	0.96	1.47±0.08	6.5±0.4
MW37	36° 33.045′ N/118° 11.604′ W	2289	Moraine crest	0.97	2.16±0.08	9.0±0.3
Tuttle moraine (M1)						
MW39	36° 32.866′ N/118° 11.462′ W	2411	Moraine crest	0.97	4.33±0.15	16.4±0.6
MW40	36° 32.877′ N/118° 11.462′ W	2396	Moraine crest	0.97	1.89±0.10	7.3±0.4
MW41	36° 32.882′ N/118° 11.462′ W	2403	Moraine crest	1.00	3.73±0.09	13.9±0.3

[a]The concentration uncertainty is based on the AMS precision to one standard deviation. The ages were calculated using 5 cm thickness for the sample.

slopes, so were not sampled for dating purposes. No evidence was found for other glacier limits between ca 2600 m and the bouldery terminal moraines in the upper cirques at ca 3600 m.

4.2. Tuttle Creek

Lateral moraines occur on both sides of Tuttle Creek, terminating close to its junction with the north fork (Fig. 3). The moraine on the south-east side of the creek forms a continuous, massive ridge that descends from ca 2500 m to 2240 m asl. The moraine is sharp-crested in its upper part, but lower down much of it is degraded. A higher moraine fragment occurs on this side of the creek at an altitude of ca 2600 m asl, at the top of a rock slope that rises above the main moraine. Three boulders from the main moraine crest yielded surface exposure ages of ~7.3–16.4 ka (M1: Table 1, Fig. 4). The wide spread of dates probably reflects the progressive exhumation of boulders during degradation of the moraine, and in such cases the true moraine age is equal to or older than the oldest date (Putkonen and Swanson, 2003). Although it is possible that the older ages reflect inheritance of TCNs, the morphostratigraphic similarity of the Tuttle and Whitney Portal moraines suggests that both formed contemporaneously at the Tioga maximum.

The moraine on the north-west side of Tuttle Creek is complex in form. Discontinuous moraine fragments trend obliquely downvalley from ca 2800 m asl to the valley floor at ca 2200 m asl, but discordances in the altitude of adjacent fragments suggest that they probably represent more than one glacial stage. The lowest portion of the moraine drops steeply in altitude, then bends sharply eastward along the north bank of Tuttle Creek where it forms a sub-horizontal ridge composed entirely of large boulders without any interstitial matrix. Well sorted clusters of cobbles and small boulders occur in several places. This openwork character is in striking contrast with the other moraines in the lower Tuttle valley and elsewhere along the Sierran range front, and suggests that this lower stretch of moraine may have been winnowed by running water subsequent to deposition. To the west of the lower Tuttle moraine, on the south-eastern slopes of Lone Pine Peak, a large rock avalanche deposit descends to the valley floor, causing the north fork of Tuttle creek to divert around its base. From the toe of the deposit, a bouldery terrace slopes downvalley, terminating at a channel between the northern (ice-distal) flank of the lower moraine and the valley side. The field relations suggest that deposition of the terrace and modification of the lower moraine may have occurred during a flood event that originated in the north fork of the Tuttle valley, possibly associated with the drainage of a lake dammed by the landslide deposit. Surface exposure dates for four boulders from the crest of the lower moraine range from 6.5 to 9.0 ka (M1': Table 1, Fig. 4).

5. Fan morphology and chronology

5.1. Lone Pine fan

The Lone Pine fan has a broadly conical form with a convex cross profile and a concave long profile, with slopes declining from 5.5° near the apex to 3.5° where the lower fan abuts the Alabama Hills (Blair, 2002; Figs. 5 and 6). The upper and middle parts of the fan are incised by a gorge now occupied by the underfit Lone Pine Creek, which is flanked by inset terraces (Qg4; Bierman et al., 1995). On either side of the incised gorge, the fan surface (Qg3) is occupied by a system of large palaeochannels and boulder deposits, which exhibit systematic changes in morphology downfan. On the *upper fan*, above ca 1900 m

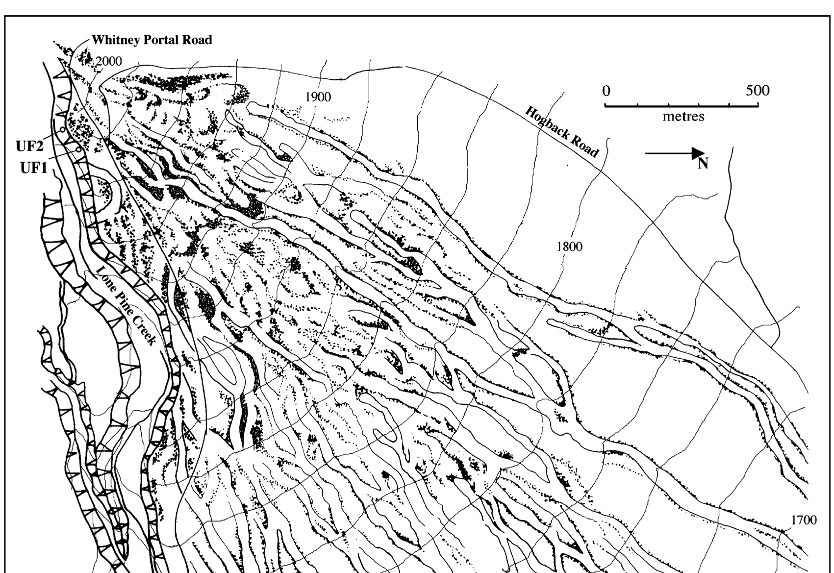

Fig. 5. Map of the upper Lone Pine fan, showing bouldery channel margins, levees, and lobes (stipple pattern).

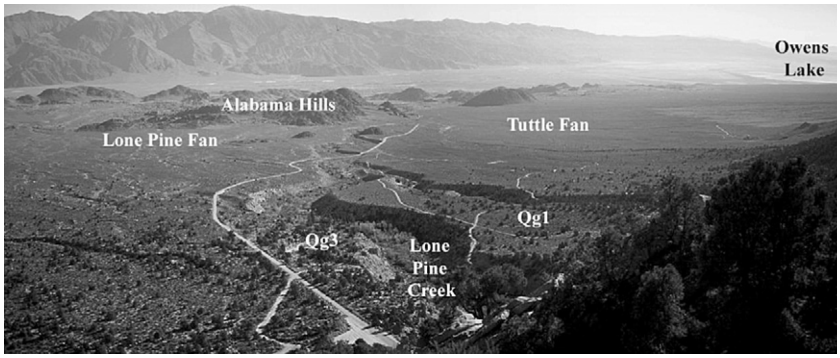

Fig. 6. View from Whitney Portal, showing the upper Lone Pine fan, the Alabama Hills, and Owens Lake.

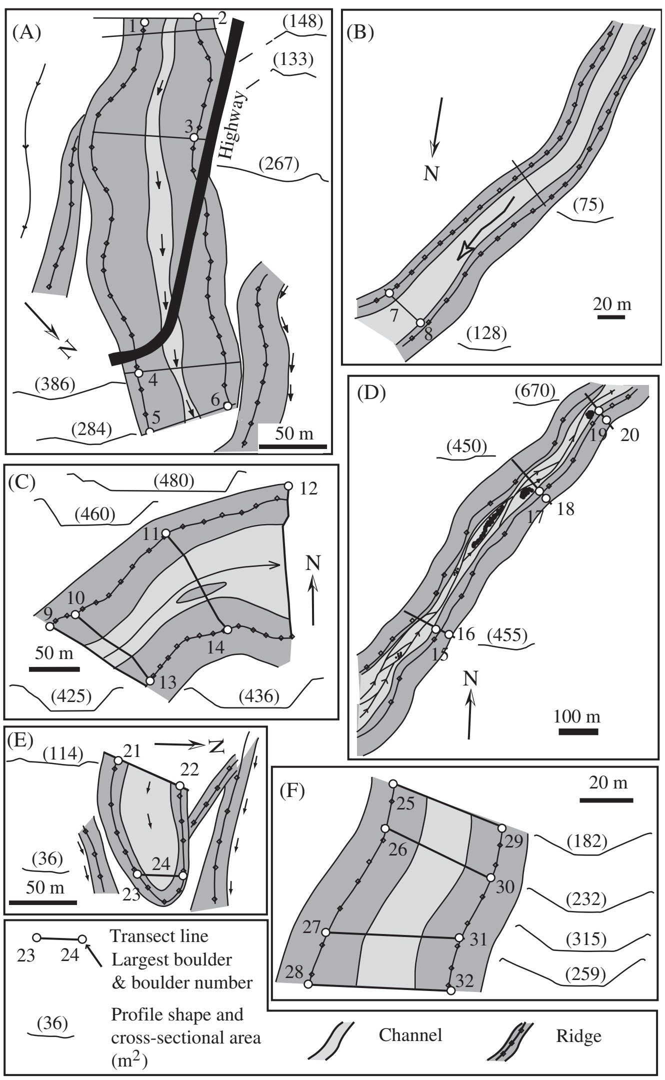

Fig. 7. Geomorphic maps showing selected channel reaches in the upper and middle reaches of the Lone Pine fan.

asl, channels are typically 50–100 m across and 5–10 m deep, and banked by levées of large boulders (Figs. 5, 7 and 8A). The channels typically originate in blind heads several hundreds of metres downfan from the apex. Some channels extend to the lower parts of the fan, but several terminate on the upper fan in steep-fronted boulder lobes (Figs. 5 and 7E). Transverse lobes of openwork boulders occur in inter-channel areas (Fig. 8B).

On the *middle fan*, between ca 1900 and 1700 m asl, the channels form a complex braided network separated by longitudinal islands and bar forms (Fig. 5). As on the upper fan, several channels originate in blind heads. Channel confluences are almost invariably graded, without breaks of slope in either channel. At channel difluences, side-branches generally split off at a higher level than the main channel floor. The largest channels are 120 m across and 15 m deep, but shallower, chute-like forms are common. Most channels are bounded by boulder levées, although these are generally lower than those on the upper fan, and are commonly only one boulder high. Transverse and longitudinal boulder bars occur between channels, and mid-channel longitudinal boulder bars occur in several places. The bar shown in Fig. 8C is over 200 m long, and consists of imbricated boulders up to 3 m long. With distance downfan, the interchannel areas become increasingly less bouldery, and appear to represent relict fine-grained fan deposits that have been incised by the channel system.

On the *lower fan*, below ca 1700 m asl, channels become fewer, as a result of both channel confluence and progressive channel shallowing and termination. There is evidence of local overdeepening where channels abut rocky outliers of the Alabama Hills, locally forming deep scours up to 12 m deep. Boulders are infrequent in interchannel areas, but in places longitudinal spreads of large boulders occur, including boulders of Sierran granodiorite 5–8 m across, and exceptionally up to 15 m. In its lowest reaches, the Lone Pine fan diverges around the Alabama Hills, splitting into a broad northern branch and a narrow southern branch which passes through a gap in the Alabama Hills to meet the Owens Valley near the town of Lone Pine (hereafter termed the *Lone Pine gap*; Fig. 3). The northern branch consists of two levels; an upper surface littered with very large weathered boulders (Fig. 8D), and a lower, less weathered surface alongside Hogback Creek. Boulder weathering on the upper surface

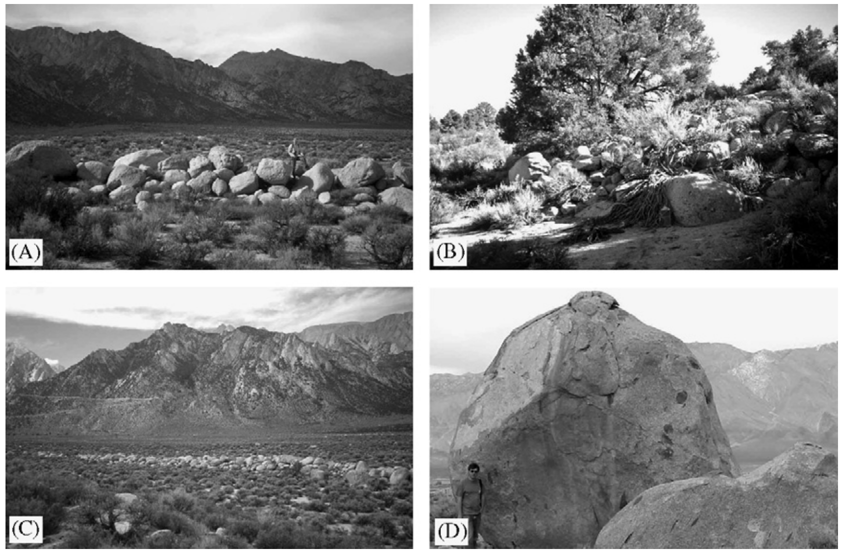

Fig. 8. Views of surface forms on the Lone Pine fan. A: Channel margin levee, upperfan. Note boulder imbrication (flow from left to right); B: transverse lobe front, upper fan. Note sorting of boulders; C: Longitudinal mid-channel bar, mid-fan; D: boulder of Sierran granodiorite, lower fan, north branch. This boulder is located ~10 km from the nearest bedrock source, and yielded a surface exposure age of MW15.

is typically very advanced, and in several places, phenocrysts, aplite veins and xenoliths stand up to 30 cm proud of granular boulder surfaces. Some boulders are completely planed off at ground level, and others have 'mushroom-like'' forms with ground-level pediments and tafoni. The lower, less weathered fan surface consists of channels with bouldery, open framework levées and bouldery interfluves. Some very weathered boulders occur, similar to those on the upper surface. The southern branch of the Lone Pine fan converges with part of the lower Tuttle fan, and is described in detail in Sections 2.

The main upper and mid-fan surfaces correspond to surface Qg3 of Bierman et al. (1995). Most of the adjusted surface exposure dates from this surface are in the range 23–32 ka yr BP (^{10}Be), with one older outlier of ~42 ka (Fig. 4). The true age of the surface is inferred to be ~23–32 ka, with the older date reflecting boulder inheritance. Bierman et al.'s (1995) dates from Qg1 show considerable spread, ranging from ~50 to 142 ka (^{10}Be; Fig. 4). The large spread of ages indicates that boulder exhumation and/or surface weathering have been significant.

We collected additional samples from boulders on the upper, older surface of the northern branch of the Lone Pine fan (Fig. 3), focusing on upstanding aplite veins and xenoliths on very large boulders (>3 m high) to minimise uncertainties associated with boulder weathering and exhumation. The three dates cluster around 84 ka BP. The dates, however, cannot represent the true age of the whole of the Qg1 surface because four of the five dates obtained by Bierman et al. (1995) are considerably older than ~100 ka. Anomalously old dates can indicate boulder inheritance, but it is highly unlikely that the majority of boulders on Qg1 contain significant inherited ^{10}Be, as this is clearly not the case for boulders on other parts of the Lone Pine and Tuttle fans (Fig. 4). We infer that Qg3 has a complex depositional history involving the transport of large boulders on more than one occasion, although current data are insufficient to determine the number or age of these events partly because of the influence of boulder weathering and exhumation.

Bierman et al. (1995) obtained 5 dates for the inset surface Qg4, adjusted values of which lie in the range 1.1–1.8 ka (^{10}Be; Fig. 4). This surface is littered with large boulders, but because the surface is inset it is likely that the boulders were derived from older flood deposits. It is probable that Qg4 represents Holocene reworking of the fan, rather than a late-stage flood event.

5.2. Tuttle fan

The Tuttle fan is morphologically similar to the Lone Pine fan, with a convex cross profile, a concave long profile, extensive networks of anastomosing flat-floored channels flanked by boulder levées, and a deeply incised gorge occupied by inset terraces and the present-day underfit stream (Fig. 9). There are also important differences, however. First, the north-west lateral margin of the fan consists of a steep, bouldery bluff which increases in height upfan, but diminishes a little towards the apex (TP 1–3, Figs. 9 and 10). At the apex itself, at an altitude of 1900 m asl, the fan margin takes the form of a large bouldery levée, which has a maximum height of ~3 m on its proximal side and ~12 m on its distal side (TP 4 & 5, Fig. 10). Above the fan apex, the levée diminishes rapidly in height and merges with a broad terrace with a system of shallow palaeochannels on its surface. An equivalent terrace occurs on the south side of the valley, but no levée is present at the fan apex.

Second, many of the channel, levée and bar forms on the upper part of the Tuttle fan differ from those on the Lone Pine fan (Figs. 5 and 9). Extending downfan in a

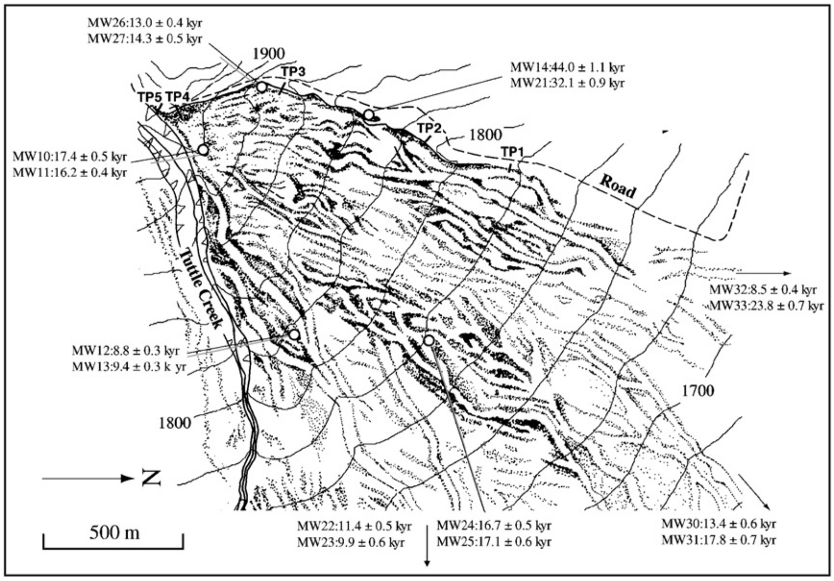

Fig. 9. Map of the upper Tuttle fan, showing bouldery channel margins, levees and lobes (stipple), surface exposure sampling sites (small circles) and ages, and the location of the surveyed profiles (TP1 to TP5) shown in Fig. 10.

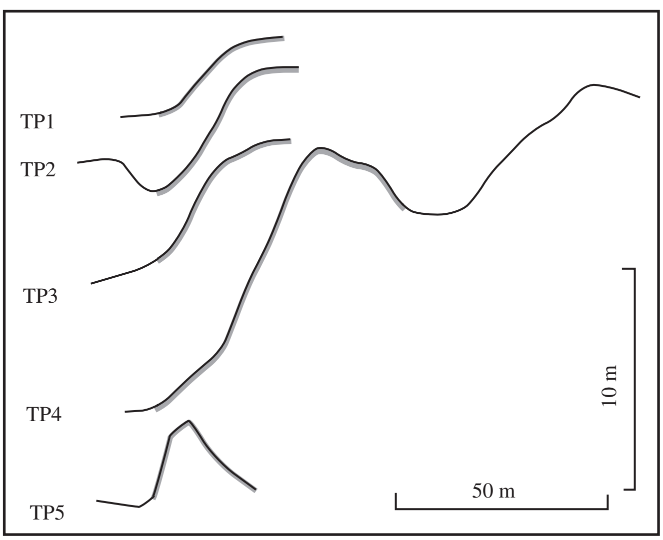

Fig. 10. Profiles across the northern margin of the Tuttle fan.

north-easterly direction from near the apex is a striking complex channel network, consisting of tortuous, anastomosing channels separated by crescent-shaped boulder bars. Some of the boulders are very large (up to 6 m long axis), and locally form imbricated clusters. The channels are typically 50 m wide and 10 m deep, and locally deepen where they bifurcate around crescentic bars. Channel junctions are generally graded, and the network forms a coherent pattern which appears to have formed simultaneously. Elsewhere on the fan surface, channels form simpler dendritic networks, some of which can be traced for many km downfan. Some of the channel systems have graded junctions, but in several places channel segments are truncated or overprinted by others, indicating multiphase formation.

A third difference between the upper Tuttle and upper Lone Pine fans is the presence on the former of flat-topped, open-work boulder tongues that splay off channel margins or out of channel mouths (Figs. 9, 10 and 11A,B). These features typically have steep lateral and frontal margins, with fronts standing several metres above the general fan surface. Most exhibit striking size sorting and upward fining.

Sixteen cosmogenic surface exposure dates were obtained from boulders on the upper Tuttle fan (Table 1, Figs. 4 and 9). Viewed together, the dates suggest at least two depositional events: an older one at ~32–44 ka BP, and a younger one at ~8–18 ka BP. The spatial distribution of the dated boulders, however, suggests that the younger event can be subdivided further. First, in 5 out of 7 cases, pairs of closely spaced boulders yielded very similar dates, suggesting that exposure ages are not spatially random, as would be the case if all variability was attributable to differential weathering, exhumation and inheritance. Second, boulder age distribution is compatible with the relative age of fan surface features as determined from geomorphological evidence. For example, two pairs of dates were obtained from the anastomosing channel network in the centre of the fan; the upper pair gave ages of 16.2 and 17.4 ka BP, whereas the lower pair yielded dates of 16.7 and 17.1 ka BP, a close clustering compatible with formation of the channel network in a single event around 17 ka BP. In contrast, younger dates were obtained from two pairs of boulders in levées and lobes associated with a dendritic channel system on the southern side of the fan (8.8 and 9.4 ka and 9.9 and 11.4 ka). The denditic channel system cross-cuts the anastomosing network near its upper end, and is therefore demonstrably younger. Thus, at least three distinct depositional events are represented on the upper Tuttle fan, at ~9–13, 16–18, and 32–44 ka BP. A date pair of 13.0 and 14.3 ka from near the north-western margin of the fan may represent a fourth event, but the evidence is insufficient to rule out alternative interpretations.

The mid-fan zone on the Tuttle fan is similar to that on the Lone Pine fan, and consists of broad inter-channel areas with scattered boulders and boulder clusters, incised by large u-shaped channels flanked by boulder levees (Figs. 11C and D). Like the Lone Pine fan, the lower Tuttle fan bifurcates and passes through gaps in the Alabama Hills. The southern branch consists of a bouldery terrace above the lower part of Tuttle Creek, which winds through a narrow gorge (the Tuttle gap, Fig. 3). At the eastern end of the Tuttle gap, where it debouches into Owens Valley, the terrace feeds into a fan which has numerous channels and intervening boulder bars on its surface. The fan descends to an altitude of ~1160 m, where it disappears beneath lacustrine deposits.

The northern branch of the lower Tuttle fan converges with the lower Lone Pine fan near the upper (western) end of the Lone Pine Gap (Fig. 3). Where the fans meet, the surface of the Tuttle fan is inset below the Lone Pine fan surface indicating that, at this locality at least, it is the younger of the two. The inset Tuttle surface grades downvalley to the east into bouldery terraces standing either side of Lone Pine Creek, whereas the Lone Pine fan surface is erosionally truncated and does not extend far into the gap. The terrace surfaces are occupied by a series of channels and boulder bars. At its lower end, the terrace on the north side of the gap crosses a low pass to the north and grades into the ‘‘faulted fan’’ dated by Bierman et al. (1995); Figs. 4 and 11. Boulders of Sierran granodiorite 2–4 m long axis are common on the surface of the faulted fan, and form a series of longitudinal bar forms (Fig. 11).

Four recalibrated dates from the faulted fan cluster in the range 9.2–12.3 (^{10}Be), with one older outlier of 19.9 ka (^{10}Be) (Bierman et al., 1995; Fig. 4). The four clustered dates are closely similar to a date obtained for a boulder on the inset surface of the lower Tuttle fan at the western end of the Lone Pine gap (MW 29; Fig. 4), which is compatible with the geomorphological evidence that the faulted fan and inset fan surfaces are correlatives. Furthermore, these dates are closely similar to those from the dendritic channel network on the upper fan, indicating that deposits of a depositional event at ca 9–13 ka BP can be traced the full length of the Tuttle fan.

6. Palaeohydrological analysis

On the basis of boulder size and channel dimensions on the Tuttle and Lone Pine fans, Blair (2001, 2002) concluded that the fan surfaces record catastrophic outburst floods, a conclusion supported in the present study. In an attempt to quantify the discharges involved, we selected six study areas from the upper and middle reaches of the Lone Pine fan (Fig. 7) and on the surface of the ‘‘faulted fan’’ in the Lone Pine gap (Fig. 12). The Lone Pine fan sites represent surface Qg3 of Bierman et al. (1995), deposited around 23–32 ka BP (Fig. 4 and Table 1), and the faulted fan sites represent the youngest flood event from the Tuttle catchment, dated to ~9–13 ka BP. This allowed us to estimate the palaeo-discharges for two separate flood events.

On the Lone Pine fan, selected channels were chain surveyed and levelled to produce geomorphic maps and a

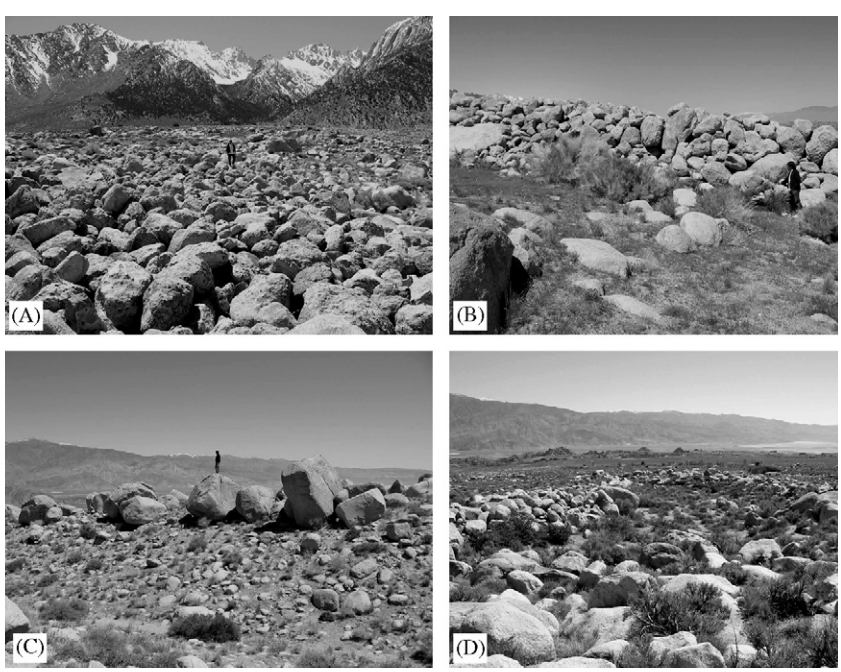

Fig. 11. Views of surface forms on the Tuttle fan. A: Top of boulder lobe, with sorted boulders ~1 m in diameter; B: Margin of lobe shown in (A); C: Channel margin levee, mid fan; D: Channel and marginal levées, mid fan.

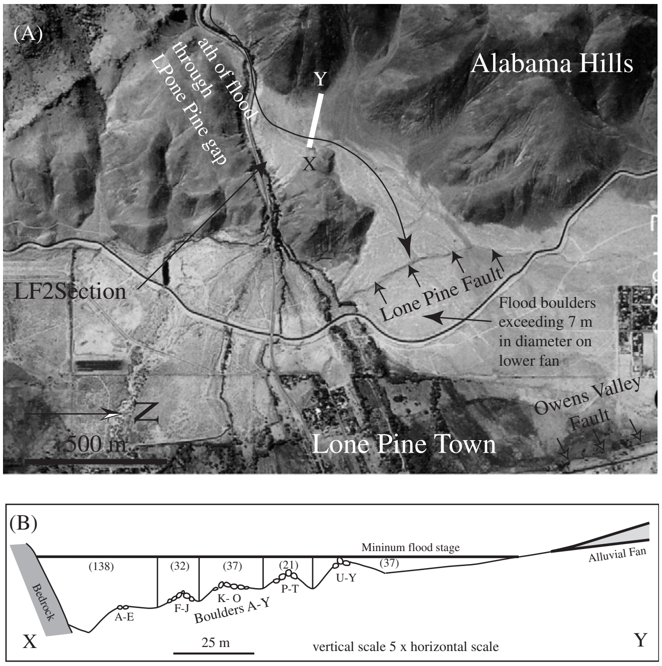

Fig. 12. (A) Aerial photograph showing the lower part of the Lone Pine gap through the Alabama Hills, and the "faulted fan" of Bierman et al. (1995); (B) profile across the deposit. The numbers in parenthesis are the calculated cross-sectional areas for channel sections between longitudinal bars.

series of profiles. The profiles were then used to calculate the minimum cross-sectional area of each channel by determining the area beneath a horizontal line projected from the highest levee/ridge to above the corresponding levee/ridge on the opposite side of the channel. Boulder *a*-, *b*- and *c*-axis of the largest boulder/s present along the transect profiles were measured (Fig. 7). On the faulted fan, a single transect was chain surveyed. Minimum flood cross-sectional area was determined by projecting a horizontal line from the highest longitudinal bar to the hillsides that constrained the flood on either side of the deposit. The *a*-, *b*- and *c*-axis of the five largest boulders on each longitudinal bar were recorded (Fig. 12).

Using the boulder size and shape data, we employed empirical functions (Costa, 1983 [Eqs. (8) and (10)] and Mears, 1979 [Eq. (7)]) to calculate the palaeovelocity required to entrain/move the boulders within the flood deposit (Tables 2 and 3). Palaeodischarges within channels on the Lone Pine fan were calculated using the minimum cross-sectional area and the palaeovelocity based on the boulder sizes. We quote the mean discharge and discharges based on individual boulders within each transect for the channels (Table 2). For most channels, the discharge is in the order of several $10^3\,m^3\,s^{-1}$. We have not attempted to estimate the total discharge across the Lone Pine fan surface because we could not confidently determine the total number of channels that were occupied simultaneously. Nevertheless, the clear evidence that multiple channels were occupied at the same time (e.g. graded channel confluences) indicates that the total discharge was »$10^3\,m^3\,s^{-1}$. Estimates of the discharge on the faulted fan are based on summing the discharge between longitudinal bars within the measured transect (Fig. 12 and Table 3), and shows that flood discharge was at least several $10^3\,m^3\,s^{-1}$.

The palaeodischarge estimates, therefore, indicate that on at least two occasions flood discharges were on the order of 10^3–$10^4\,m^3\,s^{-1}$. The occurrence of channels and boulders of similar high dimensions on the other flood surfaces we have identified strongly suggests that floods of this magnitude occurred several times during the last 100,000 years or more.

7. Sediment exposures and stratigraphy

7.1. Lower fan: Lone Pine gap

Extensive road cuts expose the fan deposits in the Lone Pine gap through the Alabama Hills. As noted above, the upper surface of the deposits at this locality can be traced upvalley to a Tuttle fan surface, which is inset below the Lone Pine fan (Figs. 3 and 12). At section LF1, near the upper (western) end of the gap, two vertical profiles were measured 105 m apart (Fig. 13). The relative elevations of the two sections were established by levelling, and the vertical scales of both profiles employ the same arbitrary datum. Both profiles show three facies associations: (1) boulder beds; (2) interbeds of gravel, granule gravel, and sand; and (3) matrix-supported diamicts. Three *boulder beds* are present (B1–B3). All are laterally extensive, clast supported, and contain weathered boulders of biotite monzogranite (derived from the Alabama Hills) and weathered and unweathered granodiorite boulders (derived from the Sierra Nevada) with an interstitial coarse sand matrix. Boulder long axes are up to 1.5 m (B1) and 2 m (B2 and B3). Bed B3 is equivalent to the deposit exposed on the terrace surface, and larger boulders (up to 4 m long axis) are present within a few tens of metres of the sections. Bed B2 can be traced continuously between the profiles, and is approximately horizontal throughout. Bed B1 only crops out in the lower (eastern) part of the exposure.

The *gravel, granule gravel and sand facies* form tabular and channelised units, typically several meters to tens of meters in lateral extent. The sand units (Sh) are horizontally stratified and poorly sorted, with scattered granules or pebbles. In places, they grade upwards into horizontally stratified granule-gravels (GRh). The gravel facies are variably clast- and matrix-supported (Gcm, Gmm). Most gravel units are structureless apart from weak imbrication in places, and some coarsen or fine upwards. The *diamict* units form laterally extensive tabular bodies, with non-erosive or welded contacts with the underlying facies. All observed units are matrix-supported, with sandy or silty–sand matrix. Some units are massive, but in many places stratification is picked out by variations in clast concentration or by sand horizons.

Interpretation: The three facies associations record contrasting sediment transport regimes. First, the clast-supported

Table 2
Boulder shape and size data, and palaeoentrainment velocity calculated using the methods of Mears (1979) and Costa (1983) for the channels shown in Fig. 7. The discharge across individual channels is calculated using the channel cross sectional areas shown in Fig. 7 and the mean paleoentrainment velocity based on boulders within the channels

Boulder number	*a*-axis (m)	*b*-axis (m)	*c*-axis (m)	Entrainment velocity for individual boulders using the methods of Costa (1983; Eq. (8)) ($m\,s^{-1}$)	Entrainment velocity for individual boulders using the methods of Costa (1983; Eq. (10)) ($m\,s^{-1}$)	Entrainment velocity for individual boulders using the methods of Mears (1979; Eq. (7)) ($m\,s^{-1}$)	Mean entrainment velocity for individual boulders using the methods of Costa (1983) and Mears (1979)[a] ($m\,s^{-1}$)	Mean discharge for individual channel sections based on individual boulders and channel cross-sectional area ($m^3\,s^{-1}$)
1	5	3	2.8	6.9	8.9	8.2	8.0±1.0	1200±200
2	2.5	1.5	1.2	5.0	6.3	5.7	5.7±0.7	800±100
3	3.8	3.0	2.2	6.9	8.9	7.5	7.7±1.0	2100±300
4	0.8	0.6	0.5	3.3	4.1	3.4	3.6±0.4	1400±200
5	1.7	1.4	1.0	4.9	6.1	5.0	5.3±0.7	1500±200
6	1.9	1.6	1.1	5.2	6.5	5.3	5.7±0.7	1600±200
7	4.1	2.4	2.1	6.2	8.0	7.3	7.2±0.9	900±100
8	3.1	2.1	1.0	5.8	7.5	6.2	6.5±0.9	800±100
9	2.0	2.0	2.0	5.7	7.3	6.1	6.4±0.8	2700±300
10	2.6	1.8	0.7	5.5	6.9	5.6	6.0±0.8	2600±400
11	5.0	3.0	2.7	6.9	8.9	8.1	8.0±1.0	3700±500
12	5.0	3.0	2.0	6.9	8.9	7.9	7.9±1.0	3800±500
13	1.7	1.3	1.3	4.7	5.9	5.2	5.3±0.6	2300±300
14	5.0	3.0	2.6	6.9	8.9	8.1	8.0±1.0	3700±500
15	2.5	2.3	2.3	6.1	7.8	6.6	6.8±0.9	3100±400
16	2.5	2.3	2.3	6.1	7.8	6.6	6.8±0.9	3100±400
17	2.2	2.0	1.8	5.7	7.3	6.0	6.4±0.8	2900±400
18	2.2	2.0	1.8	5.7	7.3	6.1	6.4±0.8	2900±400
19	3.0	2.5	2.3	6.3	8.1	7.0	7.1±0.9	4800±600
20	2.0	1.5	1.0	5.0	6.3	5.3	5.5±0.7	3700±500
21	3.3	2.1	1.8	5.8	7.5	6.7	6.7±0.8	800±100
22	1.5	0.9	0.6	4.0	4.9	4.3	4.4±0.5	500±100
23	1.2	0.9	0.9	4.0	5.0	4.3	4.4±0.5	200±20
24	2.4	1.5	0.6	5.0	6.3	5.3	5.5±0.7	200±20
25	3.0	2.0	1.5	5.7	7.3	6.3	6.5±0.8	1200±100
26	2.4	2.0	1.8	5.7	7.3	6.2	6.4±0.8	1500±200
27	5.0	3.0	2.6	6.9	8.9	8.1	8.0±1.0	2500±300
28	4.0	3.0	1.2	6.9	8.9	7.1	7.6±1.1	2000±300
29	3.0	2.0	1.5	5.7	7.3	6.3	6.5±0.8	1200±100
30	2.0	2.4	1.8	6.2	8.0	6.2	6.8±1.0	1600±200
31	3.0	3.0	1.0	6.9	8.9	6.6	7.4±1.3	2300±400
32	4.0	3.0	1.2	6.9	8.9	7.1	7.6±1.1	2000±300

[a]Error is expressed as a standard deviation.

boulder beds represent three separate episodes of high fluvial discharge, the most recent of which (B3) is represented by the fan surface and dated to ~8–12 ka BP (i.e. the youngest Tuttle fan flood event). Second, the gravel and sand facies are typical of braided stream deposits deposited by fluctuating flows, and are similar to glacifluvial outwash deposits of the Scott type described by Miall (1978). Third, the diamict facies are interpreted as debris flow deposits, similar to those deposited on fan surfaces in the south-western USA under present-day conditions. There is no consistent successional relationship between the boulder beds, gravel and sand facies, and the debris flow deposits. At the upper site, bed B2 occurs within a succession of gravels, and diamict deposits only occur near the top of the section. In contrast, at the lower site, bed B2 is sandwiched between debris flow units, and gravels only occur in one thin bed 2 m above B2. These relationships suggest that the gravel and diamictic associations have complex three-dimensional geometry, and do not represent discrete styles of deposition which simply alternated in time and simultaneously affected all parts of the valley floor. (Fig. 13)

Section LF2 is located ca 1100 m east of LF1, ca 400 m upvalley from the eastern end of the Lone Pine gap (Figs. 3, 12 and 14). The surface above this exposure equates to the faulted fan surface of Bierman et al. (1995) and is the youngest flood event identified on the Tuttle fan. Opposite the section to the south, the ground rises steeply in rock slopes underlain by Jurassic rhyolitic tuffs. In common with LF1, the section exposes a range of boulder, gravel, sand and diamict facies, but with some important

Table 3
Boulder shape and size data (*a*-, *b*- and *c*-axis), and palaeoentrainment velocity calculated using the methods of Mears (1979) and Costa (1983) for the lowermost flood deposit shown in Fig. 12. The discharge is calculated for segments across the channel and summed to provide an estimate on the minimum discharge

Boulder Number	*a*-axis (m)	*b*-axis (m)	*c*-axis (m)	Entrainment velocity for individual boulders using the methods of Costa (1983; Eq. (8)) ($m\,s^{-1}$)	Entrainment velocity for individual boulders using the methods of Costa (1983; Eq. (10)) ($m\,s^{-1}$)	Entrainment velocity for individual boulders using the methods of Mears (1979) Eq. (7) ($m\,s^{-1}$)	Mean and entrainment velocity for individual boulders using the methods of Costa (1983) and Mears (1979) ($m\,s^{-1}$)[a]	Mean for 5 boulders using all methods ($m\,s^{-1}$)[a]	Mean discharge for each channel section ($m^3\,s^{-1}$)
A	4.3	2.3	1	6.1	7.8	7.0	7.0±0.9		
B	3.1	1.8	1.5	5.5	6.9	6.4	6.3±0.8		
C	2.3	2.0	1.0	5.7	7.3	5.8	6.3±0.9		
D	3.7	3.1	1.9	7.0	9.0	7.5	7.8±1.1		
E	2.7	1.7	1.1	5.3	6.7	6.0	6.0±0.7	6.7±1.0	920±140
F	2.6	1.7	0.9	5.3	6.7	5.8	5.9±0.7		
G	2.8	2.6	2.2	6.4	8.3	7.0	7.2±0.9		
H	3.1	2.5	1.4	6.3	8.1	6.7	7.1±0.9		
I	2.0	1.1	0.9	4.4	5.5	5.1	5.0±0.6		
J	2.8	1.7	1.3	5.3	6.7	6.1	6.1±0.7	6.3±1.1	200±40
K	1.6	1.5	1.0	5.0	6.3	5.1	5.5±0.7		
L	1.9	1.6	0.5	5.2	6.5	5.1	5.6±0.8		
M	3.1	2.5	0.7	6.3	8.1	6.4	6.9±1.0		
N	2.2	2.1	1.8	5.8	7.5	6.3	6.5±0.8		
O	2.2	1.8	1.3	5.5	6.9	5.8	6.1±0.8	6.1±0.9	230±30
P	2.0	1.2	1.0	4.5	5.7	5.2	5.1±±0.6		
Q	1.7	1.6	1.5	5.2	6.5	5.6	5.8±0.7		
R	3.3	2.1	1.6	5.8	7.5	6.7	6.7±0.8		
S	2.8	1.6	1.4	5.2	6.5	6.1	5.9±0.7		
T	2.4	1.6	1.4	5.2	6.5	5.9	5.9±0.7	5.9±0.8	120±20
U	3.5	2.8	1.2	6.7	8.6	7.0	7.4±1.0		
V	3.9	2.8	1.5	6.7	8.6	7.3	7.5±1.0		
W	2.9	2.5	1.1	6.3	8.1	6.5	7.0±1.0		
X	2.7	2.2	1.2	6.0	7.6	6.3	6.6±0.9		
Y	3.1	1.6	1.4	5.2	6.5	6.3	6.0±0.7	6.9±1.0	260±40
								Total discharge across whole channel	1700±260

[a]Error expressed as a 1 standard deviation.

differences. In the central and right-hand parts of the section, a distinctive red, clast-supported, stratified diamict is exposed, with a maximum thickness of at least 6 m (Dcs, Fig. 14). The clasts are angular, granule- to cobble-sized fragments of local rhyolitic tuff, set in a poorly sorted sandy matrix of the same material. Crude, laterally discontinuous stratification is picked out by variations in clast size and concentration. The red diamict interfingers with units of gravel, sand, and bouldery facies. Gravel units occur at two levels of the exposure, and form sets of laterally extensive, tabular units with shallow, concave-up erosive (channelised) bases. The lower set of gravels thickens to the west, reaching a maximum thickness of ~4 m. All gravel units are massive to horizontally bedded, clast-supported and locally imbricated. Sand units occur in a few places in association with gravels, and have similar geometry.

Bouldery facies occur at the upper surface and lower down the section. The upper boulder bed is equivalent to B3 in Section LF1, and is well exposed on the surface of the "faulted fan," where it exhibits a range of longitudinal bar and channel forms. In section, it is clast-supported, with interstitial sandy matrix. The lower bouldery facies are all matrix-supported (Bmm) and grade laterally into matrix-supported diamicton with variable concentrations of boulders and smaller clasts (Dmm). Parts of some of the units have large boulders dispersed throughout their thickness, whereas other parts are normally graded, with concentrations of boulders and cobbles at the base and sandy layers at the top. Boulder lithology is dominated by Alabama Hills monzogranite and Sierran granodiorite, with minor quantities of local rock types. Some of the thinner diamict units do not contain boulders, but have clasts up to cobble size dispersed throughout.

The geometry of the diamict units is variable; some occupy channel forms cut into the underlying facies, whereas others consist of laterally extensive, tabular units that appear to have conformable lower contacts.

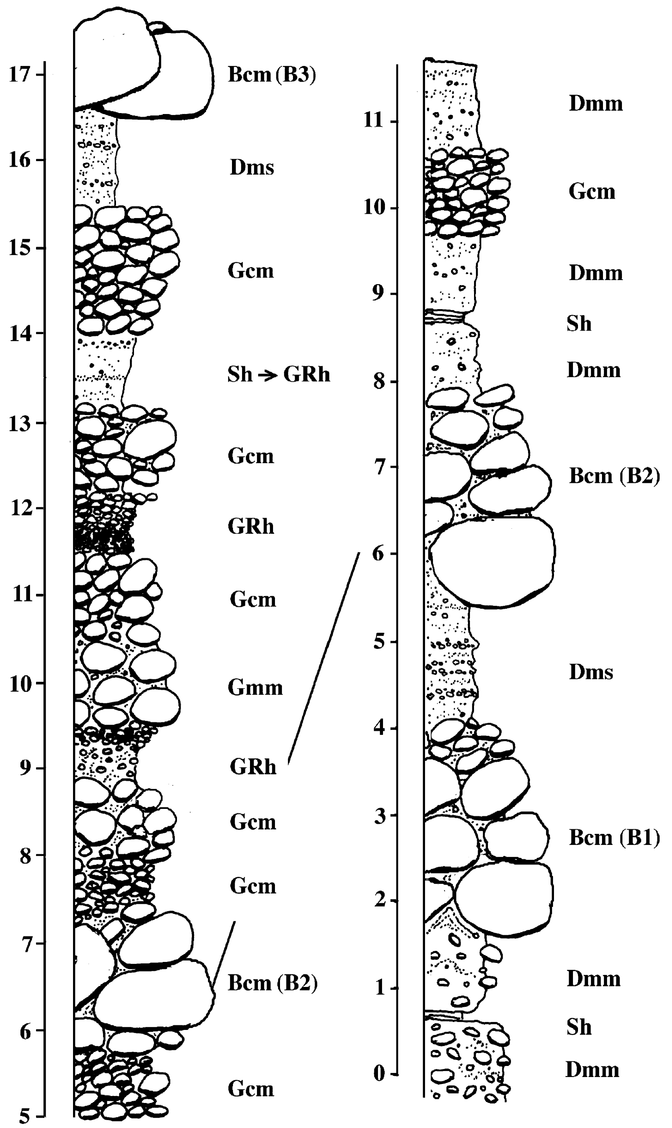

Fig. 13. Section LF1, Lone Pine gap (see Fig. 3 for the location).

Interpretation: The red clast-supported diamict is interpreted as locally derived scree, deposited at the base of the rock slope on the southern side of the Lone Pine gap opposite the section. This interpretation is supported by the presence of similar sediment in talus slopes in the area. The gravel and sand facies are similar to those exposed in LP1, and are interpreted as fluvial sediments deposited under a fluctuating flow regime. The matrix-supported boulder beds and diamicts are interpreted as debris flow deposits. Basal clast concentrations are diagnostic of low strength, fluid flows, which cannot support large clasts as suspended load (Lawson, 1979; Nemec, 1990; Coussot and Meunier, 1996; Zielinski and Van Loon, 1996). The occurrence of boulders 1–2 m across dispersed throughout some units and in some parts of others indicates that these flows had locally higher strength, and presumably lower water content. The clast supported character of the upper boulder bed, and the presence of bar and channel forms on the associated fan surface, indicates transport and emplacement by high velocity fluid flow, interpreted as a flood event. The relationship between the underlying matrix-supported bouldery debris flows and such high-discharge floods is uncertain. The large boulders of Sierran granodiorite incorporated in the units are ~10 km from the nearest possible bedrock sources, and much of that transport is likely to have been achieved in floods. However, it is unclear whether the matrix-supported debris flow deposits at LF2 were directly deposited during flood events, or whether the included boulders were reworked from flood deposits by subsequent debris flows. Because of the possibility of remobilisation and reworking, the number of flood events is uncertain at this site.

Interfingering of the red clast-supported diamict with gravel, sand, bouldery, and diamict facies indicates that talus accumulation took place during the same time frame as alternating episodes of fluvial and mass movement activity. In places, fluvial gravels and debris flow units conformably on-lap the talus, but at the right-hand end of the section a bouldery diamict unit occupies a channel cut into the talus, showing that debris flow activity was locally erosive. The evidence for contemporaneous deposition of fluvial and slope facies at LF2 is compatible with the evidence from LF1 for spatially complex patterns of

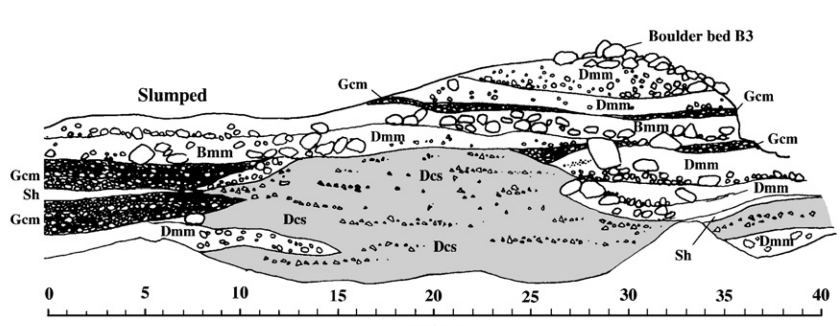

Fig. 14. Section LF2, Lone Pine gap (see Figs. 3 and 12 for the location).

deposition by fluvial and mass movement processes in the Lone Pine gap.

7.2. Lower fan: Tuttle Creek

The sediments in the south branch of the lower Tuttle Creek fan are well exposed in a roadside section (LT-1; Figs. 3 and 15). Two facies associations are present: (1) clast- to matrix-supported boulder beds; and (2) massive, clast-supported gravels with sand interbeds. Boulder beds occur at two levels, on the upper surface of the terrace and 3–5 m below the surface. The surface boulder bed is partially obscured by blown sand, and bar or channel forms were not seen at this locality, although they do occur further down-fan. The lower boulder bed contains boulders up to ~2 m long axis, and is variably clast and matrix-supported. Where the bed is clast-supported, boulders are imbricated, with upstream dipping *a*-axis and *a–b* planes. Matrix-supported parts of the bed do not have any obvious macrofabric, but exhibit normal coarse-tail grading. The matrix consists of poorly sorted gravelly silty sand. The lower contact of the lower boulder bed is an undulating erosional surface incised into underlying gravels and sands.

Gravel and sand facies also occur at two levels, above and below the lower boulder bed. The lower horizon is > 2 m thick, and consists of massive to crudely bedded cobble to small boulder gravels interbedded with horizontal and cross-bedded sand and granule facies. The upper horizon is ~3 m thick, and is composed predominantly of massive to horizontally bedded cobble gravels with occasional minor coarse sand interbeds. The gravels are invariably clast supported, with interstitial sand matrix.

7.3. Interpretation

At this site, the evidence indicates deposition by two alternating processes: (1) high discharge flood events represented by the boulder beds, and (2) moderate, alternating discharges represented by the gravel and sand facies. There is no evidence at this site for debris flow deposits.

7.4. Upper fan: Lone Pine

There are extensive, partially slumped sections near the fan apex on the north side of the gorge occupied by Lone Pine Creek (UF1, Fig. 3). A fresh exposure through the uppermost 4.5 m of the fan deposits is shown in Fig. 16. The hypermost part of the section consists of a bouldery clast- to matrix-supported unit, with boulders up to 2 m long axis. In places, the boulders are imbricated, with *a*-axes dipping up-fan. The matrix consists of coarse, poorly sorted gravelly sand. The bouldery unit grades downward into matrix-supported diamict and matrix-supported gravel. There are no distinct boundaries between the diamict and gravel components, the two only being distinguishable by lateral and vertical variations in clast content. Boulders up to 1 m long axis are scattered throughout the deposit. Clasts are locally in contact, but are more commonly enveloped in a poorly sorted sand and granule matrix. Locally, normal and inverse coarse-tail grading is present, but more commonly it exhibits a chaotic appearance. The matrix has a distinctive 'foamy' texture, with abundant small voids. At the base of the exposure is a laterally extensive boulder horizon, with clasts up to ca 1.2 m long. Clasts are angular to rounded, with a mode in the sub-rounded category. About 30% of the clasts are facetted, and a few are striated.

Blair (2002) interpreted sediments at this locality as deposits of a single outburst flood overlying basal till. None of the sediments we examined had characteristics typical of basal tills, and we conclude that all or most of the sediment exposed near the fan apex is of mass-flow origin. It is unclear, however, whether one or more events are represented.

Fig. 15. Section LT1, Tuttle gap (see Fig. 3 for the location).

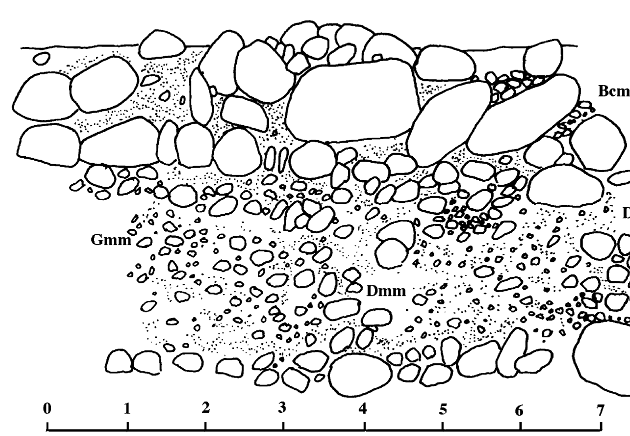

Fig. 16. Section UF1, Upper Lone Pine fan (see Figs. 3 and 5 for the location).

8. Discussion

The Tuttle and Lone Pine fans are composed of sediment deposited under three contrasting process regimes: (1) high magnitude, catastrophic floods, (2) fluvial or glacifluvial river systems, and (3) debris flows and other slope processes. Evidence for catastrophic flooding on the fans was first presented by Blair (2001, 2002), who argued that each fan surface represents a single, multi-phase event. The dating evidence presented in this paper, however, demonstrates that at least three flood events are recorded on each fan. In the Tuttle catchment, floods occurred at 9–13 ka (represented by the 'faulted fan' of Bierman et al., 1995; MW12–13, MW22–23 and MW29), at 16–18 ka (MW10–11, MW24–25, MW30–31) and at 32–44 ka BP (MW14, MW21). Another event at ~13–14 ka may be represented by MW26–27, although this is less certain than the other events. On the Lone Pine fan, flood events occurred at ~23–32 ka (Qg3: Bierman et al., 1995) and at ~84 ka (MW15–17), and an older event of indeterminate age is represented by a spread of dates up to 144 ka (Bierman et al., 1995).

None of the flood events can be confidently attributed to the failure of dated landforms which could have acted as lake dams. The 23–32 ka event on the Lone Pine fan is older than the dated lateral moraine in the catchment (MW1–5), and thus predates the most recent Tioga advance. Similarly, the 9–13 ka event on the Tuttle fan is apparently older than the 'washed moraine' in the catchment (MW34–37), although the ages ranges do overlap. The 16–18 ka event on the Tuttle fan is similar in age to the Tioga stage moraines, suggesting that it may relate to the failure of a moraine dam following ice withdrawal. However, the age of the Tioga moraines in the Tuttle catchment is not well constrained, so this suggestion remains speculative. Furthermore, although it is possible to identify multiple flood events on both fans, which presumably relate to the failure of moraine, ice, and/or landslide dams in the catchments, it is unfortunately not possible to reconstruct either the position or volume of former lakes in any case. Palaeohydrological analysis indicates that on at least two occasions, peak flood discharges were in the order of 10^3–$10^4\,m^3\,s^{-1}$. These very high discharges, and the large volume of the flood deposits (Blair, 2001, 2002), show that lake outburst floods were very efficient, episodic agents of sediment transport from the Sierra Nevada into Owens Valley.

Gravel and sand facies exposed in the lower parts of both fans record sediment transport and deposition by braided rivers. The characteristics of the deposits are similar to those of glacifluvial sediments, although current evidence is insufficient to demonstrate that they were deposited by glacial outwash. Clasts in the gravels with long axes up to 15 cm indicate episodically high discharges, implying relatively high precipitation and/or meltwater production in the Tuttle and Lone Pine catchments, and such rivers would have provided efficient means of transporting sediment from the upper catchments to the valley floor and, presumably, to Owens Lake. Debris flow and other slope deposits exposed in the lower parts of both fans record local sediment redistribution, both contemporaneously with fluvial deposition, and under relatively arid conditions. Although these processes did not directly deliver sediment to Owens Lake, they demonstrably linked slope and fluvial systems in the Alabama Hills, contributing to the remobilisation and evacuation of stored sediment.

Significantly, there is no evidence for non-catastrophic fluvial or glacifluvial deposition on the surfaces of the upper or middle Lone Pine and Tuttle fans, except adjacent to the present-day rivers. This implies that either (a) evidence of such deposits was destroyed or buried by more recent flood events, or (b) fluvial and glacifluvial sediment mainly bypassed the upper and middle parts of the fans. Possibility (a) is considered unlikely because multiple generations of flood deposits are well preserved on both fans, and we conclude that fluvial and glacifluvial activity on the upper and middle fans was dominantly non-depositional and/or erosional, with streams following narrow corridors. The dates obtained by Bierman et al. (1995) on the inset Qg4 surface on the Lone Pine fan (Fig. 4) demonstrate that, during the Holocene, non-glacial and proglacial rivers incised and reworked fan sediments previously deposited during flood events. It is likely that similar episodes of fan incision occurred during earlier times, especially following sediment deposition by floods, or when fluvial discharges were high. Direct evidence for pre-Holocene fluvial incision of pre-existing deposits is provided by section LF-2 (Fig. 14) and other exposures in the Lone Pine Gap, where sand and gravel facies truncate both locally derived scree and boulder beds containing Sierran erratics. It is therefore clear that, in addition to transporting sediment from the upper catchments, fluvial systems episodically eroded and remobilised sediment that had been previously delivered to the fans by both catastrophic flood events and non-catastrophic slope processes.

The results of this study have important implications for the interpretation of the sediment record from Owens Lake. First, on at least six occasions during the last glacial cycle, catastrophic flood events must have directly delivered glacigenic sediment from the Lone Pine and Tuttle catchments into the lake. Second, large volumes of flood-borne sediment were deposited in the fans, which were subsequently remobilised by rivers. Sediment stored in the fans could thus be delivered to Owens Lake whenever the carrying capacity of the streams was sufficiently high.

Bischoff and Cummins (2001) argued that the rock flour record from Owens Lake exhibits three levels of temporal variability, inferred to reflect glacier fluctuations on timescales of ~20 ka, 3–5 ka, and 1–2 ka. The 20 ka cycle was attributed to orbital forcing, with three major episodes of glacier expansion centred on S6/S7, S3/S2, and S1 (Fig. 17). The individual stades were attributed to glacier advances synchronous with the North Atlantic Heinrich

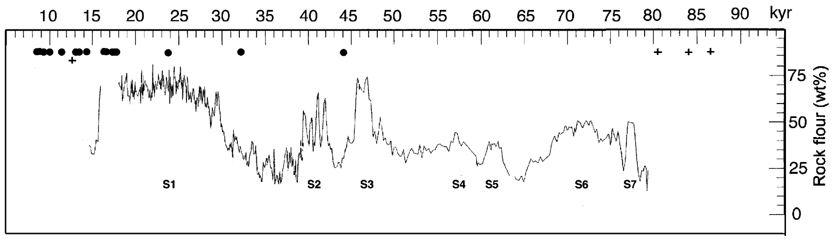

Fig. 17. The rock flour record from Owens Lake (Bischoff and Cummins, 2001), compared with surface exposure dates from boulders on the Lone Pine (crosses) and Tuttle (solid circles) fans.

events, and the rock flour peaks within or between the major stades were tentatively equated with the Greenland Dansgaard-Oeschger (D-O) oscillations. Possible correspondences between the glacio-climatic record at Owens Lake and D-O cycles have also been examined by Benson et al. (2003). The existence of such teleconnections is an intriguing possibility, but the correspondences are clearly imperfect and require rigorous quantitative testing. We argue that, although variations in glacier extent and primary production of rock flour probably occurred on all of the above timescales in the Sierra Nevada, variations in the input of rock flour to Owens Lake must also reflect processes of sediment storage and release in the intervening fan systems. This is particularly likely to be the case on the shortest timescales, i.e. rock flour fluctuations superimposed on events S1–S7 identified by Bischoff and Cummins (2001). Some fluctuations may well record glacier advances, but it is very likely that many reflect the dynamics of sediment transport in the catchments. This highlights that coarse sediment peaks in lake deposits may not simply reflect increased glaciation, but likely reflect changes in sediment storage and flux controlled by paraglacial processes.

The timing of flood events on the Lone Pine and Tuttle fans is not known with sufficient precision to allow meaningful correlation with the Owens Lake record at present (Fig. 17). Uncertainties associated with unknown boulder weathering rates and other factors mean that the actual timing of events may be offset by several millennia from our reported surface exposure dates. Moreover, it is possible that individual flood events are not registered in the published rock flour records, because of the very short duration of each event relative to the resolution of the data. Whether such events are resolved will depend critically on the thickness of each sediment pulse relative to the background sedimentation rates of 26–79 cm ka^{-1} (cf. Bischoff and Cummins, 2001). Unless flood events deposited several cm of sediment at the core site, it is more likely that the observed rock flour fluctuations reflect remobilisation of stored sediment during fan incision rather than direct input from the floods themselves. High resolution studies of the core material may allow this issue to be resolved.

In this study, we have focused on the Lone Pine and Tuttle fans, where evidence for catastrophic flooding is particularly clear. However, we have also observed large boulder-banked channels, boulder lobes, and clast- and matrix-supported boulder deposits on several other fans on the Sierran side of the Owens Lake watershed, including those in the Independence, Onion, and Horseshoe Creek catchments. On these, and many other fans in the area, streams have deeply incised and reworked sediments deposited on the fans by outburst floods and other processes. We conclude that the evacuation of rock flour from the Sierra Nevada does not simply reflect the intensity of primary glacial erosion, and that the dynamics of intervening sediment storage played a very important role in modulating the delivery of glacigenic sediment to Owens Lake.

9. Conclusion

The Tuttle and Lone Pine alluvial fans formed by a combination of sedimentation by GLOFs, fluvial and/or glacifluvial, and debris flows and other slope processes. SEDs define at least three catastrophic flood events on each fan, at 9–13 ka, 16–18 ka and 32–44 ka (Tuttle Fan); and at 23–32 ka, ~84 ka, and a poorly constrained older event (Lone Pine Fan). Sediment was likely transferred from these fan systems to Owens Lake during these depositional events/cycles. Flood sediment deposited in the fans was later removed from storage by rivers. We argue, therefore, that the millennial-scale peaks in rock flour abundance in the Owens Lake core reflect a combination of (1) fluctuations in primary subglacial erosion in the catchments in response to glacier advance–retreat cycles; (2) short-lived pulses of sediment delivered directly by catastrophic flood events; and (3) sediment released from storage in alluvial fans by fluvial and glacifluvial incision and reworking. This work emphasises that caution should taken when interpreting rock flour records and associated proxies in lake cores within or adjacent to high mountains solely as the direct effects of glaciation, because the signal is probably strongly modulated by paraglacial processes.

Acknowledgements

Many thanks to John Gosse and Peter Clark for their constructive and useful reviews on our paper. This research was funded by the National Science Foundation grant EAR-0207245 and was performed under the auspices of the US Department of Energy by the University of California, Lawrence Livermore National Laboratory under Contract No. W-7405-Eng-48.

References

Ballantyne, C.K., 2002. Paraglacial geomorphology. Quaternary Science Reviews 21, 1935–2017.

Ballantyne, C.K., Benn, D.I., 1996. Paraglacial slope adjustment during recent deglaciation: implications for slope evolution in formerly glaciated terrain. In: Brooks, S., Anderson, M.G. (Eds.), Advances in Hillslope Processes. Wiley, Chichester.

Beaty, Ch.B., 1990. Anatomy of a White Mountains debris-flow—the making of an alluvial fan. In: Rachocki, A.H., Church, M. (Eds.), Alluvial Fans: A Field Approach. John Wiley and Sons, Chichester, pp. 69–90.

Benn, D.I., Owen, L.A., 2002. Himalayan glacial sedimentary environments: a framework for reconstructing and dating former glacial extents in high mountain regions. Quaternary International 97–98, 3–25.

Benn, D.I., Kirkbride, M.P., Owen, L.A., Brazier, V., 2004. Glaciated valley landsystems. In: Evans, D.J.A. (Ed.), Glacial Landsystems. Arnold, London, pp. 372–406.

Benson, L., 2004. Western lakes. In: Gillespie, A.R., Porter, S.C., Atwater, B.F. (Eds.), The Quaternary Period in the United States. Elsevier, Amsterdam, pp. 185–204.

Benson, L.V., Burdett, J.W., Kashgarian, M., Lund, S.P., Phillips, F.M., Rye, R.O., 1996. Climatic and hydrologic oscillations in the Owens Lake basin and adjacent Sierra Nevada, California. Science 274, 746–749.

Benson, L.V., May, H.M., Antweiler, R.C., Brinton, T.I., Kashgarian, M., Smoot, J.P., Lund, S.P., 1998. Continuous lake sediment records of glaciation in the Sierra Nevada between 52,600 and 12,500 ^{14}C yr BP. Quaternary Research 50, 113–127.

Benson, L., Lund, S., Negrini, R., Linsley, B., Zic, M., 2003. Response of North American Great Basin lakes to Dansgaard-Oeschger oscillations. Quaternary Science Reviews 22, 2239–2251.

Bierman, P.R., Gillespie, A.R., Caffee, M.W., 1995. Cosmogenic ages for earthquake recurrence intervals and debris flow fan deposition, Owens Valley, California. Science 270, 447–450.

Bischoff, J.L., Cummins, K., 2001. Wisconsin glaciation of the Sierra Nevada (79,000–15,000 yr BP) as recorded by rock flour in sediments of Owens Lake, California. Quaternary Research 55, 14–24.

Bischoff, J.L., Menking, K.M., Fitts, J.P., Fitzpatrick, J.A., 1997. Climatic oscillations 10,000–155,000 yr BP at Owens Lake, California, reflected in glacial rock flour abundance and lake salinity in Core OL-92. Quaternary Research 48, 313–325.

Blair, T.C., 2001. Outburst flood sedimentation on the proglacial Tuttle Canyon alluvial fan, Owens Valley, California, USA. Journal of Sedimentary Research 71, 657–679.

Blair, T.C., 2002. Alluvial-fan sedimentation from a glacial-outburst flood, Lone Pine, California, and contrasts with meteorological flood deposits. In: Martini, I.P., Baker, V.R., Garzon, G. (Eds.), Flood and Megaflood Processes and Deposits: Recent and Ancient Examples. Special Publications of Int. Ass. Sediment., 32, pp. 113–140.

Blair, T.C., McPherson, J.G., 1998. Recent debris-flow processes and resultant form and facies of the Dolomite alluvial fan, Owens Valley, California. Journal of Sedimentary Research 68, 800–818.

Cenderelli, D.A., Wohl, E.E., 2003. Flow hydraulics and geomorphic effects of glacial-lake outburst floods in the Mount Everest region, Nepal. Earth Surface Processes and Landforms 28, 385–407.

Church, M., Ryder, J.M., 1972. Paraglacial sedimentation: a consideration of fluvial processes conditioned by glaciation. Geological Society of America Bulletin 83, 3059–3072.

Church, M., Slaymaker, O., 1989. Disequilibrium of Holocene sediment yield in glaciated British Columbia. Nature 337, 452–454.

Clague, J.J., Evans, S.G., 2000. A review of catastrophic drainage of moraine-dammed lakes in British Columbia. Quaternary Science Reviews 19, 1763–1783.

Clark, D., Gillespie, A.R., Clark, M., Burke, R., 2003. Mountain glaciations of the Sierra Neveda. In: Easterbrook, D.J. (Ed.), Quaternary Geology of the United States. INQUA 2003 Field Guide Voume. Desert Research Institute, Reno NV, pp. 287–311.

Costa, J.E., 1983. Paleohydraulic reconstruction of flash-flood peaks from boulder deposits in the Colorado Front Range. Geological Society of America Bulletin 94, 986–1004.

Coussot, P., Meunier, M., 1996. Recognition, classification and mechanical description of debris flows. Earth Science Reviews 40, 209–227.

Evans, S.G., Clague, J.J., 1994. Recent climatic change and catastrophic geomorphic processes in mountain environments. Geomorphology 10, 107–128.

Farber, D.L., Hancock, G.S., Finkel, R.C., Rodbell, D.T., 2005. The age and extent of tropical alpine glaciation in the Cordillera Blanca, Peru. Journal of Quaternary Science 20 (7–8), 759–776.

Gibbons, A.B., Megeath, J.D., Pierce, K.L., 1984. Probability of moraine survival in a succession of glacial advances. Geology 12, 327–330.

Guyton, B., 1998. Glaciers of California. University of California Press, Berkeley, CA.

Harbor, J., Warburton, J., 1993. Relative rates of glacial and nonglacial erosion in alpine environments. Arctic and Alpine Research 25.

James, L.A., Harbor, J., Fabel, D., Dahms, D., Elmore, D., 2002. Late Pleistocene glaciations in the northwestern Sierra Nevada, California. Quaternary Research 57, 409–419.

Jarrett, R.D., Costa, J.E., 1986. Hydrology, geomorphology, and dam-break modelling of the July 15, 1982 Lawn Lake and Cascade Lake dam failures, Larimer County, Colorado. US Geological Survey Professional Paper 1369, 78pp.

Kaufman, D.S., Porter, S.C., Gillespie, A.R., 2004. Quaternary alpine glaciation in Alaska, the Pacific Northwest, Sierra Nevada, and Hawaii. In: Gillespie, A.R., Porter, S.C., Atwater, B.F. (Eds.), The Quaternary Period in the United States. Elsevier, Amsterdam, pp. 77–104.

Kirkbride, M., Brazier, V., 1998. A critical evaluation of the use of glacier chronologies in climatic reconstruction, with reference to New Zealand. In: Owen, L.A. (Ed.), Mountain Glaciation. Quaternary Proceedings 6. Wiley, Chichester, pp. 55–64.

Kohl, C.P., Nishiizumi, K., 1992. Chemical isolation of quartz for measurement of in-situ-produced cosmogenic nuclides. Geochimica et Cosmochimica Acta 56, 3583–3587.

Lawson, D.E., 1979. Sedimentological analysis of the western terminus region of the Matanuska Glacier, Alaska. Cold Region Research and Engineering Laboratory, Report 79–9, Hanover, NH.

Lliboutry, L., 1977. Glaciological problems set by the control of dangerous lakes in Cordillera Blanca, Peru. II. Movement of a covered glacier embedded within a rock glacier. Journal of Glaciology 18, 255–273.

Mears, A.I., 1979. Flooding and sediment transport in a small alpine drainage basin in Colorado. Geology 7, 53–57.

Menking, K.M., 1997. Climatic signals in clay mineralogy and grain-size variations in Owens lake core OL-92, southeast California. In: Smith, G.I., Bischoff, J.L. (Eds.) An 800,000 Year Palaeoclimatic Record from Core OL-92, Owens lake, Southeast California. Geological Society of America Special Paper 317, Boulder, CO, pp. 25–36.

Miall, A.D., 1978. Lithofacies types and vertical profile models in braided river deposits: a summary. In: Miall, A.D. (Ed.), Fluvial Sedimentology. Canadian Society of Petroleum Geologists Memoir 5, pp. 597–604.

Nemec, W., 1990. Aspects of sediment movement on steep delta slopes. In: Colella, A., Prior, D. (Eds.), Coarse Grained Deltas. International Association of Sedimentologists Special Publication 10, 29–73.

Newton, M., 1991. Holocene stratigraphy and magnetostratigraphy of Owens and Mono Lakes, eastern California. Unpublished Ph.D. Thesis, University of Southern California.

O'Conner, J.E., Costa, J.E., 1993. Geologic and hydrologic hazards in glacierized basins in North America resulting from 19th and 20th century global warming. Natural Hazards 8, 121–140.

O'Conner, J.E., Hardison, J.H., Costa, J.E., 2001. Debris flows from failure of Neoglacial-Age moraine dams in the Three Sisters and Mount Jefferson Wilderness Areas, Oregon. US Geological Survey Professional Paper 1606, 93pp.

O'Conner, J.E., Grant, G.E., Costa, J.E., 2002. The geology and geography of floods. In: House, P.K., Webb, R.H., Baker, V.R., Levish, D.R. (Eds.), Ancient Floods, Modern Hazards: Principles and Applications of Paleoflood Hydrology. Water Science and Application, 5, American Geophysical Union, Washington, DC, p. 359–385.

Owen, L.A., Derbyshire, E., 1989. The Karakoram glacial depositional system. Zeitschrift fur Geomorphologie Supp.-Bd 76, 33–73.

Owen, L.A., Derbyshire, E., 1993. Quaternary and Holocene intermontane basin sedimentation in the Karakoram Mountains. In: Shroder, J.F. (Ed.), Himalaya to the Sea. Routledge, London, pp. 108–131.

Phillips, F.M., Zreda, M.G., Benson, L.V., Plummer, M.A., Elmore, D., Sharma, P., 1996. Chronology for fluctuations in late Pleistocene Sierra Nevada Glaciers and lakes. Science 274, 749–751.

Porter, S.C., Pierce, K.L., Hamilton, T.D., 1983. Late Wisconsin mountain glaciation in the western United States. In: Porter, S.C. (Ed.), Late Quaternary Environments of the United States, Volume 1, The Late Pleistocene. University of Minnesota Press, Minneapolis, pp. 71–111.

Putkonen, J., Swanson, T., 2003. Accuracy of cosmogenic ages for moraines. Quaternary Research 59, 255–261.

Reisner, M., 1986. Cadillac Desert: The American West and Its Disappearing Water. Viking, New York 564pp.

Richardson, S.D., Reynolds, J.M., 2000. An overview of glacial hazards in the Himalayas. Quaternary International 65/66, 31–47.

Small, E.E., Anderson, R.S., Repka, J.L., Finkel, R., 1997. Erosion rates of alpine bedrock summit surfaces deduced from in situ Be-10 and Al-26. Earth and Planetary Science Letters 150, 413–425.

Smith, G.I., Bischoff, J.L. (Eds.) 1997. An 800,000 Year Palaeoclimatic Record from Core OL-92, Owens Lake, Southeast California. Geological Society of America Special Paper 317.

Smith, G.I., Street-Perrott, F.A., 1983. Pluvial lakes of the western United States. In: Porter, S.C. (Ed.), Late Quaternary Environments of the United States, Vol 1, The Late Pleistocene. University of Minnesota Press, Minneapolis, pp. 190–212.

Stone, J.O., 2000. Air pressure and cosmogenic isotope production. Journal of Geophysical Research 105, 23753–23759.

Vivian R., 2001. Des Glacières du Faucigny aux Glaciers du Mont-Blanc. La Fontaine de Siloé, 298pp.

Vuichard, D., Zimmerman, M., 1986. The Langmoche flash-flood, Khumbu Himal, Nepal. Mountain Research and Development 7, 91–110.

Whipple, K.X., Dunne, T., 1992. The influence of debris-flow rheology on fan morphology, Owens Valley, California. Geological Society of America Bulletin 104, 887–900.

Yamada, T., 1998. Glacier Lake and its Outburst Flood in the Nepal Himalaya. Monograph No. 1, Data Center for Glacier Research, Japanese Society of Snow and Ice, 96pp.

Zehfuss, P.H., Bierman, P.R., Gillespie, A.R., Burke, R.M., Caffee, M.W., 2001. Slip rates on the Fish Springs fault, Owens Valley, California, deduced from cosmogenic ^{10}Be and ^{26}Al and soil development on fan surfaces. Geological Society of America Bulletin 113, 241–255.

Zielinski, T., Van Loon, A.J., 1996. Characteristics and genesis of moraine-derived flowtill varieties. Sedimentary Geology 101, 119–143.